RADIATIVE PARAMETERIZATION FOR THE FNWC GLOBAL PRIMITIVE EQUATION MODEL

Frank Wright Jenks

NAVAL POSTGRADUATE SCHOOL
Monterey, California

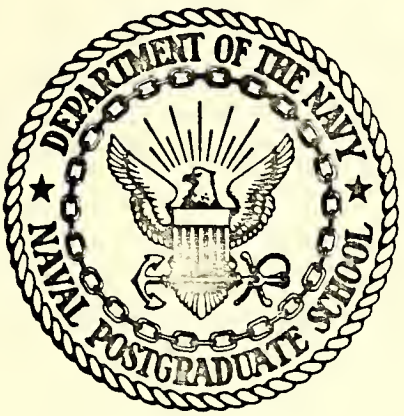

THESIS

RADIATIVE PARAMETERIZATION FOR THE
FNWC GLOBAL PRIMITIVE EQUATION MODEL

by

Frank Wright Jenks III

Thesis Advisor: F. L. Martin

March 1974

Radiative Parameterization for the FNWC Global Primitive Equation Model

by

Frank Wright Jenks III
Lieutenant, United States Navy
B.S., Miami University, 1967

Submitted in partial fulfillment of the
requirements for the degree of

MASTER OF SCIENCE IN METEOROLOGY

from the

NAVAL POSTGRADUATE SCHOOL
March 1974

ABSTRACT

This study was an evaluation of a radiational scheme for inclusion in a numerical weather prediction model. This scheme uses empirical formulations for atmospheric absorptivities, scattering and reflectivity and cloud and earth surface reflectivity to compute the solar insolation received and absorbed by the earth and key atmospheric layers. Longwave cooling by the earth is also treated with empirically derived emissivities for water-vapor and carbon dioxide. This radiation model includes a two-layer cloud parameterization scheme and calculates the effect of an additional cloud layer on previous studies.

In testing the validity of this model, use was made of Fleet Numerical Weather Central data in the form of vertical soundings on a spring day over the ocean. This data was used to calculate the radiation balance at the tropopause, the earth's surface and the key layers of the atmosphere.

TABLE OF CONTENTS

LIST OF TABLES

LIST OF FIGURES

ACKNOWLEDGEMENTS

The author wishes to express his appreciation to his wife for her support and for typing the rough draft of this thesis.

Appreciation is also expressed to the author's thesis advisor, Professor F. L. Martin, for his suggestions, advice, guidance and support in this research.

I. INTRODUCTION

This study was an attempt to produce an empirical radiative parameterization for inclusion in the Fleet Numerical Weather Central (FNWC) primitive equation prediction model.

The radiative parameters described here include two cloud layers of fractional amounts CL(1) and CL(2) at each gridpoint instead of a single cloud layer as previously used (Plante, 1973). The possibility of an additional cloud layer tends to add substantial complexity to the radiation physics, but in general this paper represents an extension of that described previously by Martin (1972). Some of the details of this radiation model are also based upon an unpublished manuscript (Martin, 1974), which in turn has some similarities to the multi-cloud models of Arakawa (1972) and Rodgers (1967).

The vertical scale used in this study was based on the five sigma ($\sigma = p/\pi$) levels of the FNWC primitive equation model. The levels in this study are called k-levels (k = 1, ..., 10). The k-levels are used for the purpose of data input as shown in Figure 1. Cloud cover is dealt with by means of a two-layer parameterization, with one high-level cloud layer from k = 4 to k = 6 and a low-level cloud deck from k = 8 to k = 9, in amounts

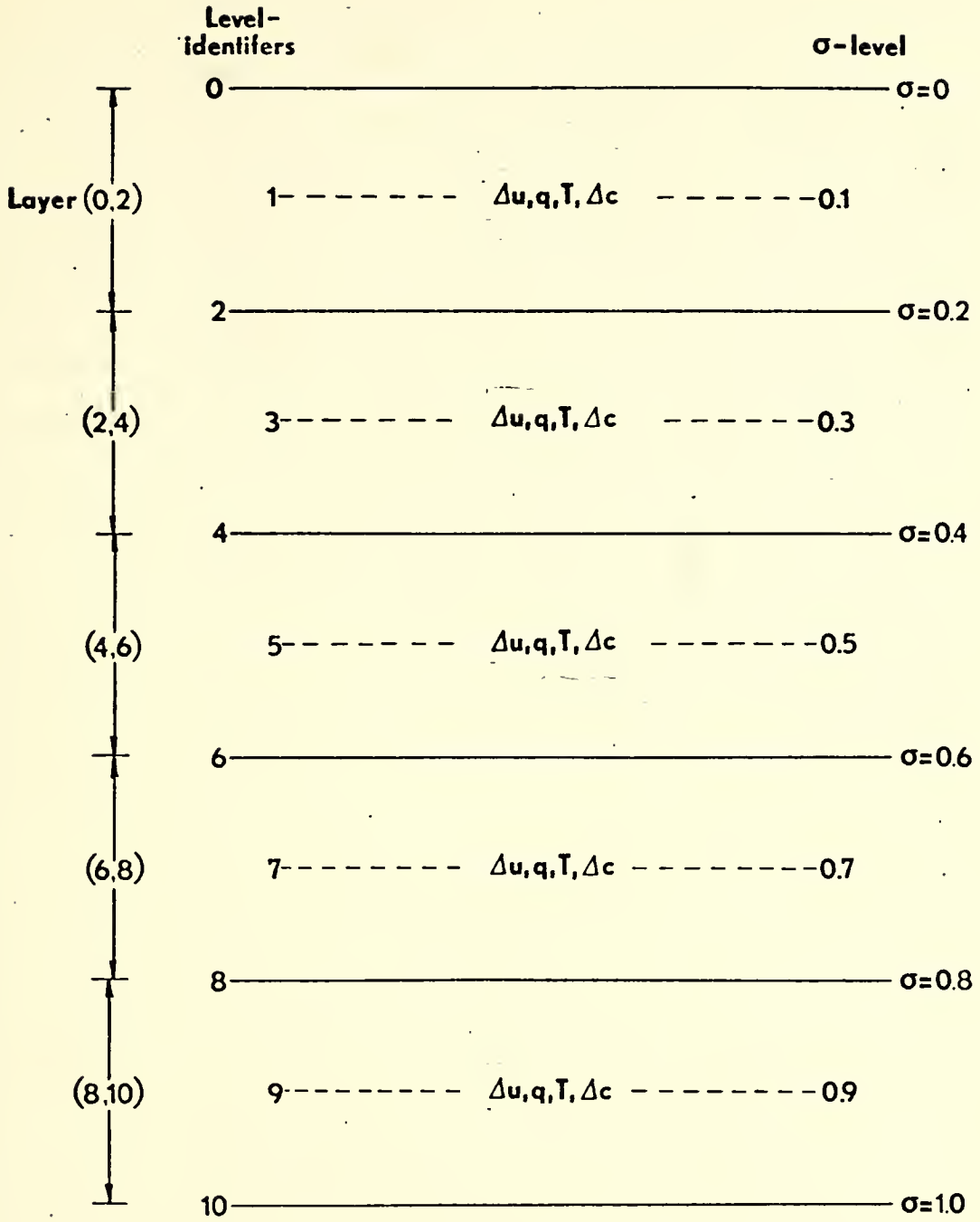

Figure 1. Five-layer radiative sounding used in this study. Levels are identified by their values on the k-scale, while layers are identified by their level boundary indices (e.g., (8, 10) in parentheses. Pressure-scaled water vapor and CO_2 mass increments ΔU and ΔC, respectively, as well as mixing ratio (q) are introduced at the odd levels while temperature is introduced at all levels.

CL(1) and CL(2), respectively. In the computations for pressure-scaled water vapor and CO_2 absorber masses a realistic method was used to extrapolate water vapor mixing ratio values above the level of k = 4, which is normally the highest moisture level available from radiosonde data. The system for computation of the net flux of terrestrial radiation makes use of new empirical absorptivities of water vapor and CO_2 (Sasamori, 1968), which are incorporated in the Martin (1974) manuscript.

To evaluate the radiative heat transfers of this study, three meridians derived from FNWC analyses were used. These meridians are all from the Pacific Ocean area and most of the radiative soundings were in the Northern Hemisphere.

II. DATA PREPARATION

The data used in this study was in the form of three meridians of 25 vertical soundings over the Pacific Ocean. These meridians were located at 125°W, 170°W and 145°E as shown in Figure 2.

The soundings on these data lines were taken from the original FNWC analyses of temperature at the surface and at nine other standard levels up to 100 millibars for 0000GMT, 25 April 1973. The six moisture values were given by the vapor pressure at sea level, and by dew-point depression for levels from 925 mb to 400 mb. Table I(a) gives as an example the original sounding at gridpoint (1, 1) in the FNWC map. The data-processing methods applied to the temperature and mixing ratio data for the determination of the water vapor and CO_2 absorber masses, and the cloud amounts within required k-level boundaries (Figure 1) are detailed in the following subsections. It should be noted that all soundings start at sea level, and as a reasonable approximation may be considered to have surface pressure $\pi \doteq 1000$ mb. Hence the k-levels of Figure 1 became 1000, 900, 800, 700, 600, 500, 400, 300, 200, and 100 mb, respectively.

A. TEMPERATURE TERMS

The temperatures were listed at each mandatory level between 1000, ..., 100 mb. The radiative sounding

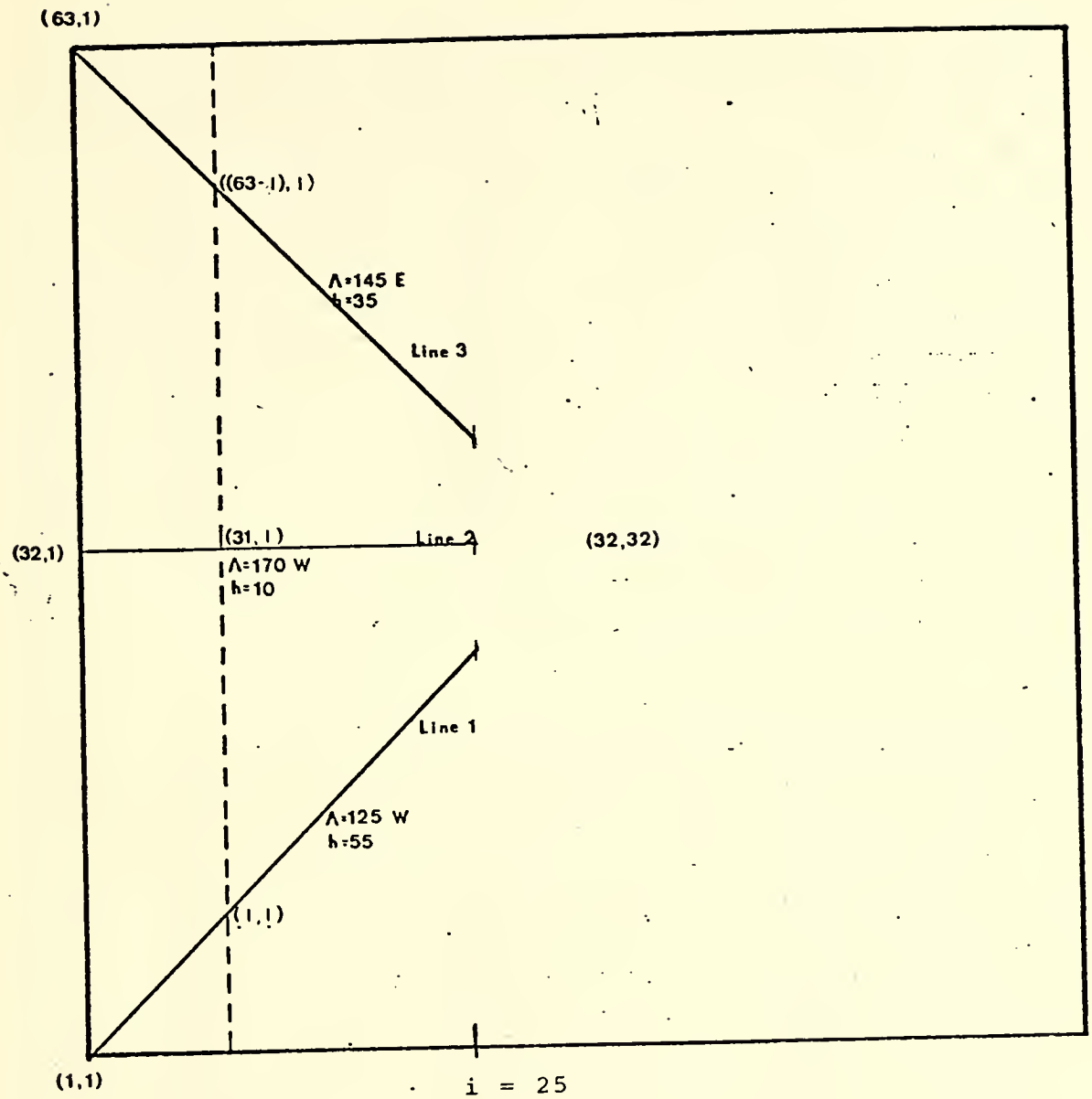

Figure 2. FNWC polar stereographic grid and meridians (1,2,3) selected for study. The longitudes Λ and hour angles of the sun relative to local noon are shown for each meridian.

TABLE I(a). Form of original FNWC grid soundings. The humidity parameter between 925, ..., 400 mb is dewpoint depression.

Pressure (mb)	T (°C)	Humidity Parameters
1000	28.5	27.7 mb
925	20.0	3.2°C
850	16.2	2.9°C
700	7.1	5.0°C
500	-9.6	4.7°C
400	-21.4	2.0°C
300	-36.4	
250	-45.3	
200	-55.5	
150	-66.9	
100	-80.3	

TABLE I(b). Form of the corresponding radiative sounding with temperature and mixing ratio listed at k-levels.

Pressure (mb)	T (°K)	Mixing Ratio
1000	299.0	18.35 $g(kg)^{-1}$
900	291.7	16.50
800	286.6	12.97
700	280.3	7.84
600	272.6	4.75
500	263.6	2.97
400	251.8	2.21
300	236.8	0.73
200	217.7	0.23
100	192.9	0.04
0	192.9	0.00

temperatures at certain k-levels were obtained by interpolation. The temperature T_{10} was set equal to the listed air temperature. At the top of the atmosphere, the temperature was assumed to be isothermal from 100 mb to p=0, with the mixing ratio also approaching zero at p=0.

The interpolation scheme used was the three-point Lagrangian formula of the form:

$$\begin{aligned} T_k = {} & T_0((P_k-P_1)(P_k-P_2))/((P_0-P_1)(P_0-P_2)) \\ & + T_1((P_k-P_0)(P_k-P_2))/((P_1-P_0)(P_1-P_2)) \\ & + T_2((P_k-P_0)(P_k-P_1))/((P_2-P_0)(P_2-P_1)) \end{aligned} \qquad (2\text{-}1)$$

Here P_0 lies above P_k, where k is the pressure level desired for T_k-interpolation, and P_1,P_2 lie below level k. For example, with k = 9, P_1 and P_2 were taken as 925 mb and 1000 mb, respectively. The parameters T_0, T_1 and T_2 are temperatures at the same levels as P_0, P_1, and P_2, respectively.

B. MOISTURE TREATMENT IN THE SOUNDING

The moisture parameters from the original sounding (Table I(a)) were converted into the mixing ratios at each of the original sounding levels. At k = 10 the surface vapor pressure, e_{air}, was used to calculate the mixing ratio by use of Equation (2-2):

$$q_{1000} \doteq .62197\ e_{air}/1000 \qquad (2\text{-}2)$$

where e_{air} is in mb.

In calculating the mixing ratios at the remaining original data levels Equation (2-3) was used (after p. 63, Fleagle and Businger, 1963):

$$q(p) = \frac{.62197\ e^{(A-\frac{B}{T})}}{p} * \exp^{[\frac{-B(T-T_D)}{T\ T_D}]}\ 1000 \qquad (2\text{-}3)$$

Here q(p) is the mixing ratio at level p.

A = 21.656

B = 5418.0°K

T = temperature at level p (°K)

T_D = dew point at level p (°K)

$T-T_D$ = dew point depression (°K)

The q-values were then interpolated to the k-levels using an equation similar to Equation (2-1). The results of this interpolation are shown in an example, Table I(b).

Accurate humidity information is not generally available at or above 300 mb. To find the q-values at k = 3, 2 and 1, an extrapolation formulation was used

$$\frac{q(p)}{q_5} = (\frac{p}{500})^{\lambda} \qquad (2\text{-}4)$$

This formula is similar to that developed by Smith (1966). However, instead of using the surface values of pressure and moisture in Equation(2-4) use was made of the pressure and moisture values at the 500 mb level. Equation (2-4) was solved for the parameter λ using the "best-fit" between the variables $y \equiv \log \frac{q}{q_5}$ and $x \equiv \log \frac{p}{500}$. This was

done by using the six values of q of each original soundings corresponding to p = 1000, 925, 850, 700, 500, and 400 of Table I(a). The "best-fit" values of λ were then used in Equation (2-4) to extrapolate the q-values to p = 300, 200 and 100 mb.

The usual formula for a best-fit parameter λ relating y_i and x_i samples is given in standard texts on statistics (e.g., Crow et al, 1960)

$$\lambda = \frac{\sum_{i=1}^{i=6} y_i x_i}{\sum_{i=1}^{i=6} x_i^2}$$

A further statistic computed in connection with each λ-profile was the correlation coefficient

$$R_{y/x} \equiv \lambda \sqrt{\frac{\sum_{i=1}^{6} x_i^2}{\sum_{i=1}^{6} y_i^2}}$$

The correlation coefficient for each λ-profile was generally in the range .95 to .99, which tended to enhance the credibility of the usefulness of the λ-profile technique.

The mean values, $\bar{\lambda}$, together with the standard deviation, $\sigma(\lambda)$, based upon the 25 soundings on each meridian are listed below:

	Meridian 1	Meridian 2	Meridian 3
$\bar{\lambda}$	3.143	3.712	2.931
$\sigma(\lambda)$	0.799	0.915	1.094

C. PRESSURE-SCALED ABSORBER MASSES

With the mixing ratios computed at each odd k-level (Figure 1), it is possible to compute the pressure-scaled water vapor absorber masses in each layer. In Figure 1, these water vapor layer-masses were denoted by ΔU, but here we develop notation which is more representative of the layers under consideration. For example, the pressure-scaled water vapor mass in layer (8, 10) is given by

$$U(8, 10) = \frac{q_9 \Delta p}{g}\left[\frac{p_9}{1013.25}\right]^{0.72} \qquad (2\text{-}5)$$

where the pressure ratio raised to the exponent 0.72 (after Möller and Raschke, 1964) has been employed. For the layer (6, 8), an analog to Equation (2-5) was employed with q_9 replaced by q_7 and p_9 by p_7. A similar procedure was followed in the topmost layers (0, 2),(2, 4) and (4, 6). Equation (2-6) affords an example for the topmost layer (0, 2).

$$U(0, 2) = \frac{q_1 \Delta p}{g}\left[\frac{p_1}{1013.25}\right]^{0.72} \qquad (2\text{-}6)$$

In each of the five layers Δp is 200 mb.

The algorithm for computing the integrated water vapor mass above the earth's surface is then as follows:

$$\begin{aligned} U(10) &= 0.0 \\ U(8) &= U(10) + U(8, 10) \\ U(6) &= U(8) + U(6, 8) \\ U(4) &= U(6) + U(4, 6) \\ U(2) &= U(4) + U(2, 4) \\ U(1) &= U(2) + .5(U(0, 2)) \\ U(0) &= U(2) + U(0, 2) \end{aligned} \qquad (2\text{-}7)$$

The principle for the computation of the carbon dioxide scaled mass is similar to that for water vapor. Here, however, it is customary to state the pressure-scaled mass in terms of the normal temperature and pressure (N.T.P.) volume over a cm^2 of the earth's surface. Thus

$$C(8, 10) = 3.14 \times 10^{-4} \left(\frac{\Delta p}{g\ \rho_s}\right) \left(\frac{p_9}{1013.25}\right)^{0.72} \qquad (2\text{-}8)$$

In (2-8), the fraction 3.14×10^{-4} is the constant mixing ratio of carbon dioxide by volume, while $\frac{\Delta p}{g\ \rho_s}$ is the N.T.P. thickness of the layer $\Delta P = P_{10} - P_8$. The quantity ρ_s is the constant density in a standard homogeneous atmosphere for which $T_s = 273.16°K$ everywhere and $p_s = 1013.25$ mb. With minor modification, Equation (2-8) becomes

$$C(8, 10) = 3.14 \times 10^{-4} (H) \left(\frac{\Delta P}{1013.25}\right) \left(\frac{P_9}{1013.25}\right)^{0.72} \qquad (2\text{-}9)$$

$$H = \frac{RT_s}{g} = 7.995 \times 10^5 \text{ cm.}$$

All other layer thicknesses of carbon dioxide are similar in form to C(8, 10), for example:

$$C(6, 8) = 3.14 \times 10^{-4} (H) \left(\frac{\Delta P}{1013.25}\right) \left(\frac{P_7}{1013.25}\right)^{0.72} \qquad (2\text{-}10)$$

The integration for the layer masses of C(8), C(6), C(4), C(2), C(1) and C(0) follow exactly the procedure outlined for water vapor.

D. CLOUD PARAMETERIZATION

In the calculations of the fractional cloud cover amounts in layers (4, 6) and (8, 9) the relative humidities and thus the saturation vapor pressure at levels k = 5 and k = 9 must be available. The saturation vapor pressures at each level were calculated using Equations (2-11(a)) and (2-11(b)), and the relative humidity using Equations (2-12(a)) and (2-12(b)):

$$q_s(500) = \frac{.62197e^{(A-\frac{B}{T_5})}}{500} \qquad (2\text{-}11(a))$$

$$q_s(900) = \frac{.62197e^{(A-\frac{B}{T_9})}}{900} \qquad (2\text{-}11(b))$$

where A = 21.656

B = 5418.0K

$$RH(5) = \frac{q(500)}{q_s(500)} \qquad (2\text{-}12(a))$$

$$RH(9) = \frac{q(900)}{q_s(900)} \qquad (2\text{-}12(b))$$

The relative humidity values were then used to calculate the fractional cloud amounts at each layer using the following formulation, which is similar to Smagorinsky's (1960):

$$CL(1) = 2.0(RH(5)) - 0.7 \qquad (2\text{-}13(a))$$

$$CL(2) = 3.33(RH(9)) - 2.0 \qquad (2\text{-}13(b))$$

III. SOLAR RADIATION

A. PARTITION OF SOLAR INSOLATION

In this study, following Joseph (1966), a solar constant of 2.00 ly min^{-1} was assumed. This is the value at the top of the atmosphere; however, it is assumed subject to a four percent attenuation by oxygen and ozone above the tropopause. Thus the effective solar constant assumed at level k = 2 in this study is 1.92 ly min^{-1}.

The effective solar insolation at the tropopause was computed from

$$F(2) = S\left[\frac{R}{R_m}\right]^{-2} \cos Z \qquad (3\text{-}1)$$

where

S = effective solar constant

Cos Z = cosine of the zenith angle

R/R_m = ratio of the actual earth-sun distance to the mean earth-sun distance.

The ratio R/R_m is listed as a function of the Julian date in the Smithsonian Meteorological Tables (List, 1958). In this study based upon data for 25 April at 0000GMT a value of R/R_m = 1.00606 was used. The cosine of the zenith angle was calculated by

$$\text{Cos } Z = \text{Sin}\phi \text{ Sin}\delta + \text{Cos}\phi \text{ Cos}\delta \text{ Cos } h \qquad (3\text{-}2)$$

where ϕ = Latitude
δ = Solar declination for April 25th = 12°56'
h = hour angle

The value of the declination was taken from Table 169 (List, 1958), and the value of Sinϕ was calculated using two different formulas depending on the data-line used for the computations. These values of Sinϕ along lines one, two, and three are calculated in terms of the FNWC map coordinates (I,J) as:

$$\text{Lines } 1,3 \qquad \text{Sin}\phi = \frac{973.752 - 2(32-I)^2}{973.752 + 2(32-I)^2} \qquad (3\text{-}3a)$$

$$\text{Line } 2 \qquad \text{Sin}\phi = \frac{973.752 - (32-I)^2}{973.752 + (32-I)^2} \qquad (3\text{-}3b)$$

$$I = 1, \ldots, 25$$

Here I is the abscissa distance on the FNWC grid, Figure 2. The soundings were all taken at 0000GMT; therefore, the value for the hour angle h, can easily be calculated. For example, in this experiment solar noon existed at the 180th meridian and the hour angles h = 55°, 10° and 35° occurred along lines one, two, and three, respectively.

Following Joseph (1966) a computationally simple partition of the solar insolation was used for this study. Joseph divided the insolation at level 2, F(2), into two parts, one of which was subject to water vapor absorption but not to Rayleigh scattering. This portion is given by

$$F(A) = 0.349F(2); \qquad (3\text{-}4)$$

the remaining portion of the insolation,

$$F(S) = 0.651F(2), \qquad (3\text{-}5)$$

is subject only to Rayleigh scattering (but not to water vapor absorption) in a clear moist atmosphere. The presence of two cloud decks in this study introduces cloud-reflectivity into both the F(A) and F(S) solar energy portions.

The F(S) energy is composed of all wavelengths $\lambda \leq$ 0.9 μm since here water-vapor absorption is negligible. The F(A) portion consists of those wavelengths $\lambda > 0.9$ μm where absorption by water-vapor and carbon dioxide bands in the near infra-red is the dominant attentuation process in clear air.

B. DISPOSITION OF F(S) INSOLATION

Joseph (1966) found that empirical values of Rayleigh clear-sky albedo, (after Coulson, 1959), were best-fit using the least squares technique by the following formula

$$\alpha(R) = .085 + .25074 \left[\log_{10} \left(\frac{\pi}{p_0} \text{ Sec } Z\right)\right] \qquad (3\text{-}6)$$

$$p_0 = 1013.25$$

Here $\pi/p_0 \doteq 1$ in view of the fact that mean sea level occurs near 1000 mb. The value Sec Z is equal to $(\text{Cos } Z)^{-1}$, where Cos Z is calculated from (3-2).

Another reflective-type parameter which must be considered in this study is the surface albedo α(G). Over

the land areas of the Northern Hemisphere a constant average surface albedo of 0.14 is utilized. However, the value over the oceans depends on cos Z. Since in this study all of the soundings were over the ocean, the equation

$$\alpha(G) = \max \{.06, .06 + .54\ (.7 - \cos Z)\} \quad (3\text{-}7)$$

was used to calculate $\alpha(G)$, (after Gates et al, (1971)).

Since a two-layer cloud model was used, four separate cloud cases are discussed below.

1. Clear Sky Case

In this case the F(S) insolation is subject only to Rayleigh sky reflectivity, $\alpha(R)$, and the earth-surface reflectivity, $\alpha(G)$, of Equations (3-6) and (3-7). Considering the possibility of multiple reflections between the earth and atmosphere, each of which diverts downward the fraction $\alpha(R)$ of the earth's surface reflectance $\alpha(G)$, the clear sky insolation at the earth's surface after scattering is given by

$$ISl0(0,0) = F(S)[1-\alpha(R)][1-\alpha(G)]/[1-\alpha(R)\alpha(G)] \quad (3\text{-}8)$$

In the next three cases, where clouds were present, the cloud reflectivity values suggested by C. D. Rodgers (1967) were used. Thus for the higher level clouds (between k = 4 and 6), R(1)= 0.54 and for the lower level clouds (between k = 8 and 9), R(2) is 0.66.

2. Cloudy Sky Cases

We consider first the fraction of the grid area having clouds at both levels. The F(S) insolation absorbed by the ground at such a grid point is given by

$$ISlO(1,1) = F(S)[(1-R(1))(1-R(2))(1-\alpha(G))] \quad (3\text{-}9)$$
$$*[1-((R(1)R(2)+R(2)\alpha(G)+R(1)\alpha(G))$$
$$+ 2(R(1)R(2)\alpha(G))]^{-1}$$

(after Arakawa,1972). The special symbols (1,1) denote CL(1) = CL(2) = 1.0, which will temporarily be assumed.

The other cloud-cover variations to be considered are those of CL(1) = 1.0, CL(2) = 0.0 and CL(1) = 0.0, CL(2) = 1.0, respectively. In the former case, R(2) = 0.0 in (3-9) so that

$$ISlO(1,0) = F(S)(1-R(1))(1-\alpha(G))/(1-R(1)\alpha(G)) \quad (3\text{-}10)$$

In the latter case with clouds at the lower layer only it follows that

$$ISlO(0,1) = F(S)(1-R(2))(1-\alpha(G))/(1-R(2)\alpha(G)) \quad (3\text{-}11)$$

Equations (3-8), (3-9), (3-10), and (3-11) were used to calculate the absorbed F(S) insolation at the earth's surface after only reflective-type processes are considered to take place. However, in each case the sky was considered to be either overcast or clear and an appropriate grid-area weighting scheme was necessary to correct to the actual cloud conditions CL(1), CL(2).

3. The Weighted F(S) Insolation

The cloud combinations denoted by (0,0), (1,1), (1,0), and (0,1), respectively, actually occur with the areal coverage (or weights) at a grid point given by the following functions:

$$\begin{aligned} W(0,0) &= (1-CL(1))(1-CL(2)) \\ W(1,1) &= (CL(1))(CL(2)) \\ W(1,0) &= (CL(1))(1-CL(2)) \\ W(0,1) &= (1-CL(1))(CL(2)) \end{aligned} \qquad (3\text{-}12)$$

at each grid point.

When these weights were applied multiplicatively in sequence with the right sides of Equations (3-8), (3-9), (3-10), and (3-11), then the composite surface-absorbed insolation, IS10 resulted.

$$IS10 = IS10(0,0)W(0,0) + IS10(1,1)W(1,1) + IS10(1,0)W(1,0) + IS10(0,1)W(0,1) \qquad (3\text{-}13)$$

Note that by subtraction of IS10 from F(S) we also arrive at that portion of the F(S) insolation reflected to space.

C. DISPOSITION OF F(A) INSOLATION

In the following sections, the fraction of the insolation which is absorbed by atmospheric water-vapor and carbon dioxide is discussed.

1. The Clear Sky Case

In this connection the Manabe-Möller absorptivity function

$$\underline{a}(2,2k) = .271[U(2,2k)\,\mathrm{Sec}\ Z]^{0.303} \qquad (3\text{-}14)$$

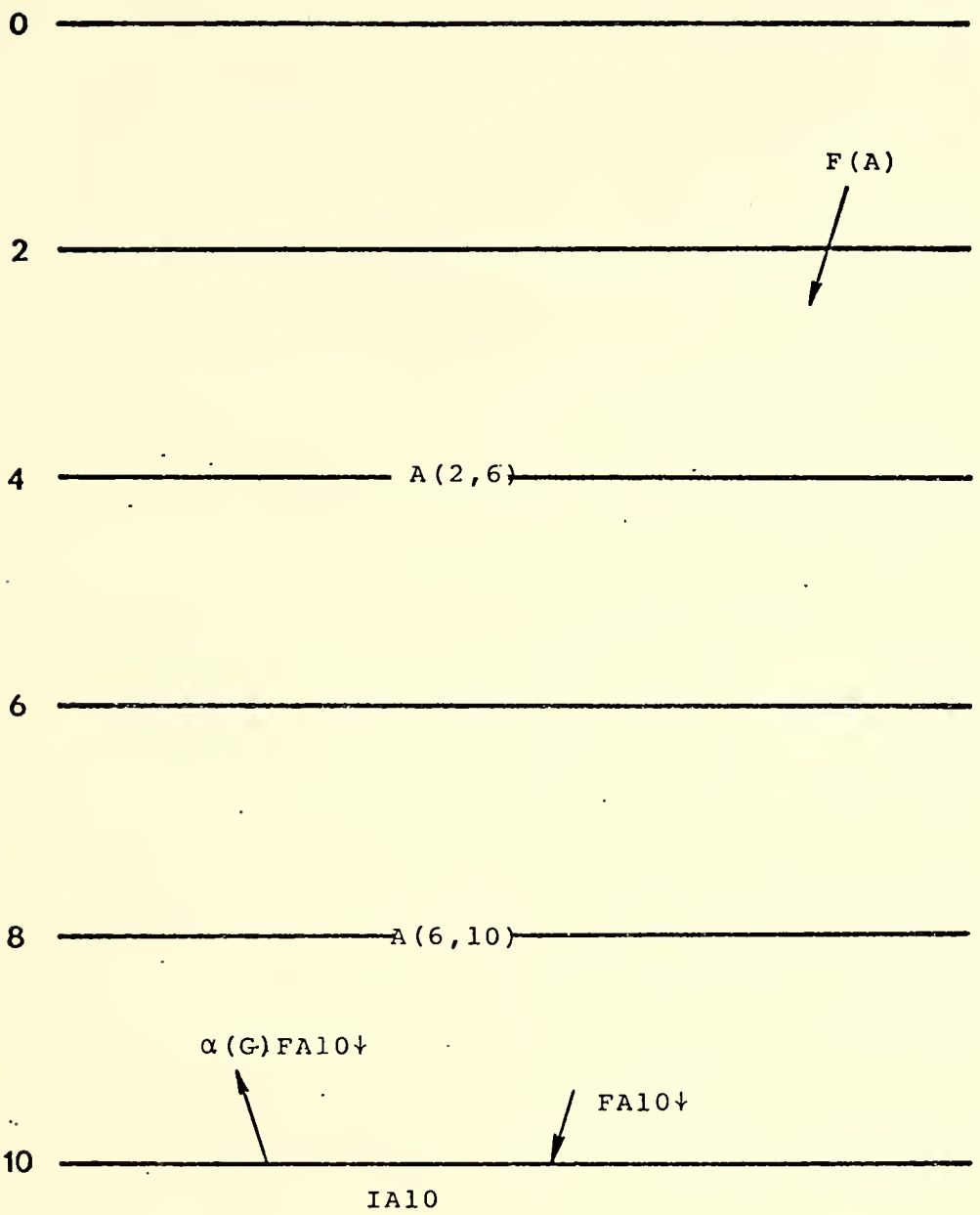

Figure 3. Schematic representation of F(A) insolation disposition in the clear sky case.

was used. The form of Equation (3-14) indicates that the absorptivity a is applied over the pressure-scaled water-vapor mass between levels 2 and 2k (see Figure 1) along the zenith slant-path angle Z. Therefore, assuming negligible water-vapor mass above level 2, the absorbed solar insolation in the layer (2,6) is

$$A(2,6) = 0.271F(A)[U(2,6)\text{Sec } Z]^{0.303} \qquad (3\text{-}15)$$

Similarly, the absorbed insolation in the layer (2,10) is

$$A(2,10) = 0.271F(A)[U(2,10)\text{Sec } Z]^{0.303} \qquad (3\text{-}16)$$

and the absorbed insolation in the layer (6,10) is given (see Figure 3) by

$$A(6,10) = A(2,10) - A(2,6) \qquad (3\text{-}17)$$

The direct transmission of F(A) insolation to the earth's surface was found by subtracting A(2,10) from F(A). This direct transmission is partially reflected by the earth's surface (the value computed for $\alpha(G)$ in Equation (3-7) is applicable here) and the remainder, absorbed at the earth's surface, is given by

$$IA10(0,0)=F(A)\{1-.271[U(2,10)\text{Sec } Z]^{0.303}\}(1-\alpha(G)) \qquad (3\text{-}18)$$

In the following subsections dealing with partially cloudy layers, it is necessary to adopt representative cloud reflectivities. For this purpose, values suggested

by C. D. Rodgers (1967) were used. These reflectivity values for the F(A) wavelengths differ from those listed by Rodgers for the F(S) wavelengths. We followed the procedure of considering overcast cloud conditions whenever clouds occur and subsequently applying the weighting factors as was done in Section III(B).

2. Overcast in Both Cloud Layers

Here, with clouds at both levels the cloud reflecivity values RA(1) = .46 and RA(2) = .50 were used. In addition Rodgers suggests cloud absorptivities of A(1) = .20 and A(2) = .30 (see Figure 4). With the following set of formulas, the downward directed insolations FA4↓, etc., were calculated at each required level in order to arrive at a value for the insolation abosrbed by the atmospheric layers, and finally by the earth's surface.

$$A(2,4)' = F(A).271[U(2,4)\text{Sec } Z]^{0.303} \quad (3\text{-}19a)$$

$$FA4\downarrow = F(A)[1-.271(U(2,4)\text{Sec } Z)^{0.303}] \quad (3\text{-}19b)$$

$$A(2,4)'' = F(A)RA(1).271[U(2,4)\text{Sec } Z]^{0.303} \quad (3\text{-}19c)$$

$$A(2,4) = A(2,4)' + A(2,4)'' \quad (3\text{-}19d)$$

$$A(4,6) = FA4\downarrow A(1) \quad (3\text{-}19e)$$

$$FA6\downarrow = FA4\downarrow(1-RA(1)-A(1)) \quad (3\text{-}19f)$$

$$FA8\downarrow = FA6\downarrow(TD(6,8))[1-RA(1)RA(2)(TD(6,8))^{2}]^{-1} \quad (3\text{-}19g)$$

$$A(6,8) = FA6\downarrow - FA8\downarrow \quad (3\text{-}19h)$$

$$A(8,9) = FA8\downarrow A(2) \quad (3\text{-}19i)$$

$$FA9\downarrow = FA8\downarrow(1-RA(2)-A(2)) \quad (3\text{-}19j)$$

$$FA10\downarrow = FA9\downarrow TD(9,10)[1-\alpha(G)RA(2)(TD(9,10))^{2}]^{-1} \quad (3\text{-}19k)$$

$$A(9,10) = FA9\downarrow - FA10\downarrow \quad (3\text{-}19\ell)$$

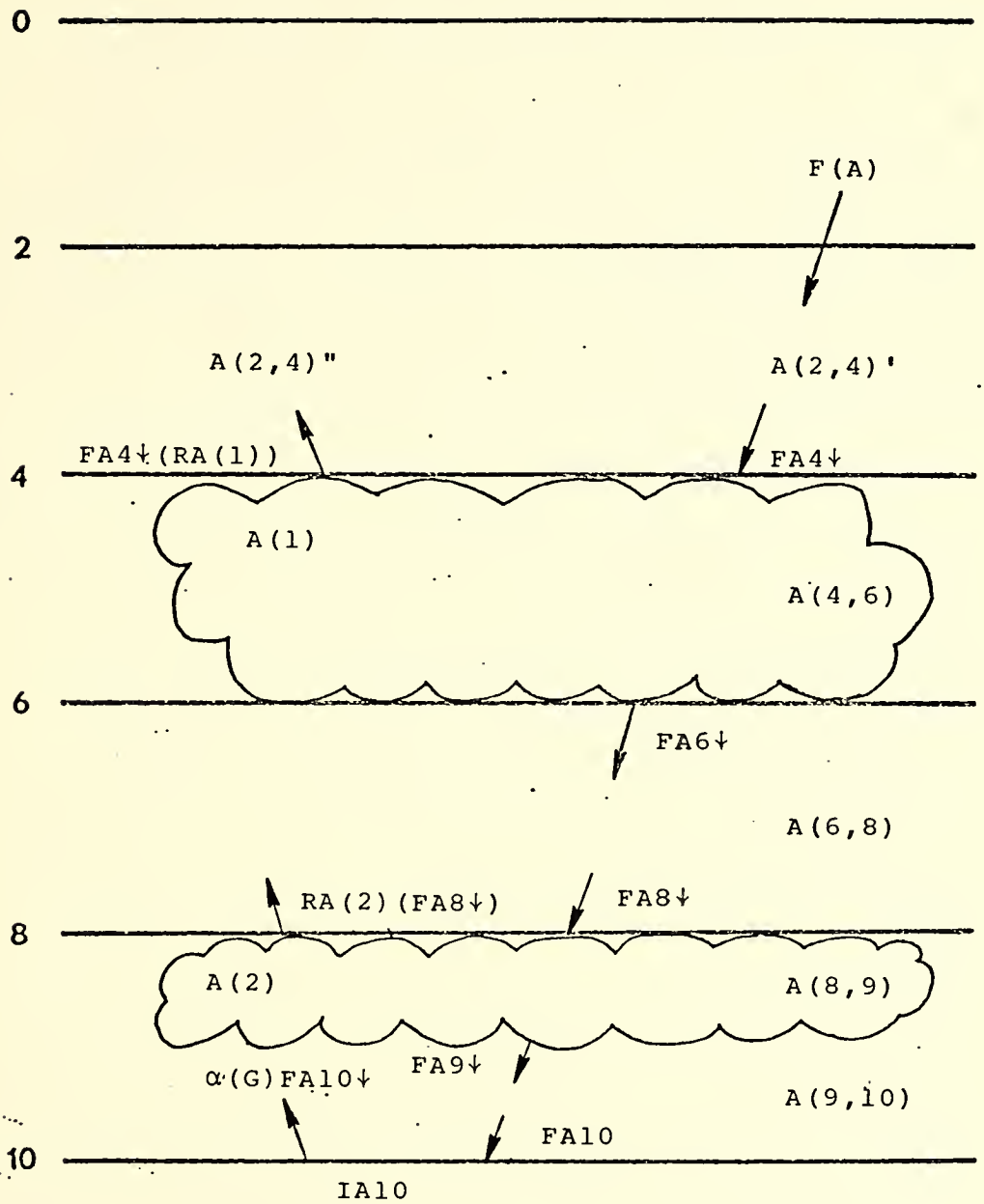

Figure 4. Schematic representation of F(A) insolation disposition in the case of two overcast layers.

where

$$TD(6, 8) = 1 - .271[U(6,8)5/3]^{0.303} \qquad (3\text{-}20)$$

$$TD(9, 10) = 1 - .271[U(9,10)5/3]^{0.303}$$

In the preceding equations A(2, 4), A(4, 6), A(6, 8), A(8,9), and A(9,10) represent the insolation absorbed in the indicated layers. A superscript prime following A(2,4) indicates absorption (by use of Equation 3-14) of the downward directed beam, while the double prime indicates absorption of the beam specularly reflected upward from the cloud top. The functions of Equation (3-20) represent transmissivity after diffuse passage through a cloud or sub-cloud layer, which causes the effective replacement of Sec Z in Equation (3-14) by $\overline{\text{Sec } Z} \doteq 5/3$ (Katayama, 1966). The symbols FA6↓, FA8↓, FA9↓, and FA10↓ indicate the downward streams of insolation passing through the indicated levels. Note that the effect of multiple reflections between clouds is incorporated in the denominator of FA8↓, while that between the lower cloud and the ground has a corresponding term in the denominator of FA10↓, involving the reflectivities $\alpha(G)$ and RA(2). The effect of the multiple reflectances as modeled here is to enhance the insolation at the lowermost reflecting boundary of the two under consideration.

Finally, note that the flux absorbed by the earth's surface under the conditions of an overcast layer at both levels is given by

$$IA10(1,1) = FA10(1-\alpha(G)) \qquad (3\text{-}21)$$

3. Disposition of F(A) Insolation with an Upper Overcast

In this case with only an upper overcast layer, the values of RA(1) and A(1) used are the same as those of the preceding section. However, a somewhat simpler set of disposition equations result:

$$A(2,4) = F(A)\{.271[U(2,4)\,\mathrm{Sec}\,Z]^{0.303} + [1 - .271(U(2,4)\,\mathrm{Sec}\,Z)^{0.303}]RA(1)\} \quad (3\text{-}22a)$$

$$A(4,6) = F(A)A(1)[1 - .271(U(2,4)\,\mathrm{Sec}\,Z)^{0.303}] \quad (3\text{-}22b)$$

$$FA6\downarrow = F(A)[1 - .271(U(2,4)\,\mathrm{Sec}\,Z)^{0.303}][1 - RA(1) - A(1)] \quad (3\text{-}22c)$$

$$FA10\downarrow = FA6\downarrow[1 - .271(U(6,10)5/3)^{0.303}] * [1 - \alpha(G)RA(1)TD(6,10)^{2}]^{-1} \quad (3\text{-}22d)$$

$$A(6,10) = FA6\downarrow - FA10\downarrow \quad (3\text{-}22e)$$

Here the variables are defined similarly to those of the preceding section. (Note that A(2, 4)' and A (2, 4)" have been combined in Equation (3-22) to give A(2, 4) and the definition of TD(6, 10) is similar in principle to that of TD(6, 8)). The absorbed insolation at the ground is given by

$$IA10(1,0) = FA10\downarrow (1 - \alpha(G)) \quad (3\text{-}23)$$

(see Figure 5).

4. Disposition of F(A) Insolation with a Low Overcast

The set of equations which describe the behavior of the insolation with a low overcast deck are given below (see Figure 6).

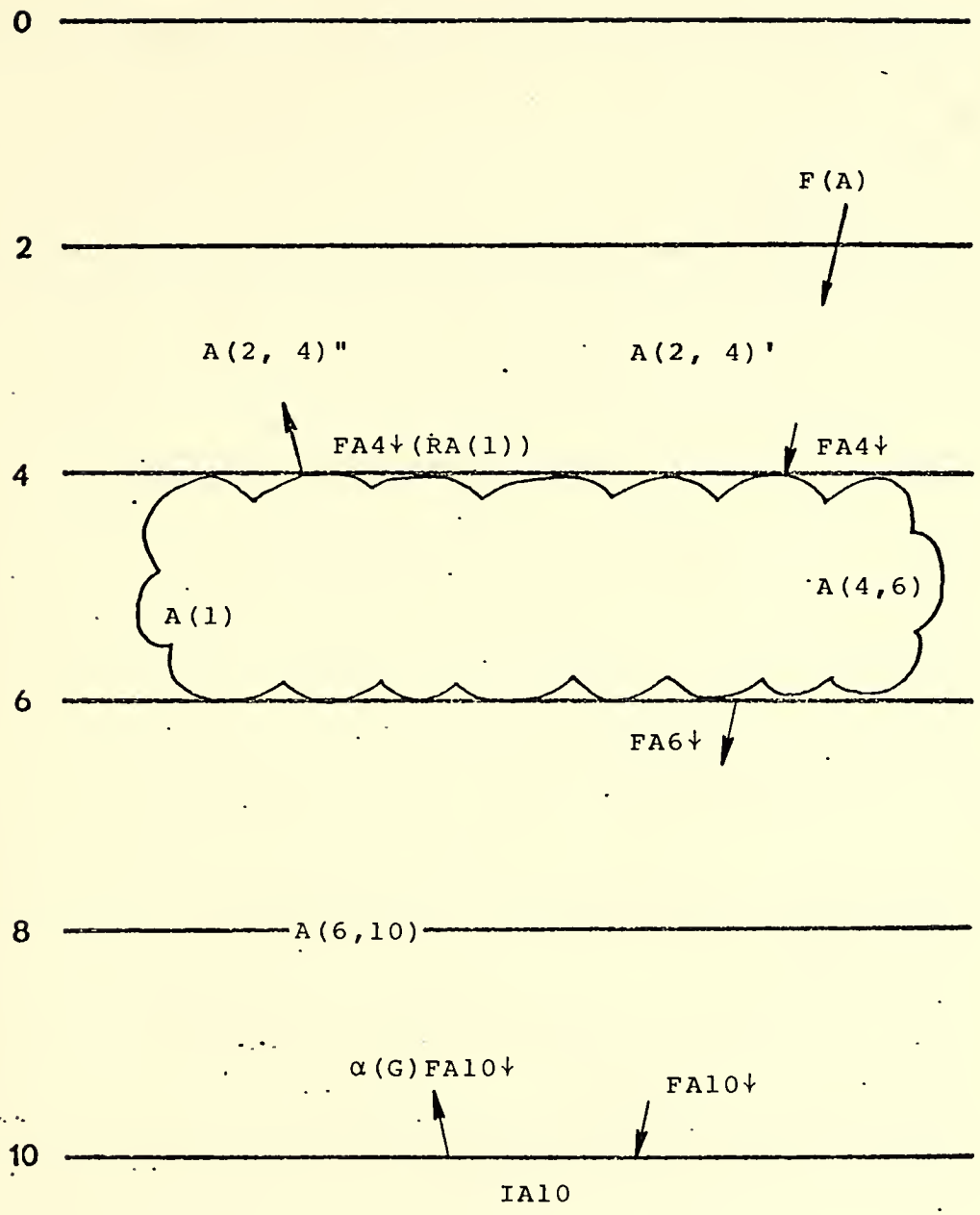

Figure 5. Schematic representation of F(A) insolation disposition with an upper overcast layer only.

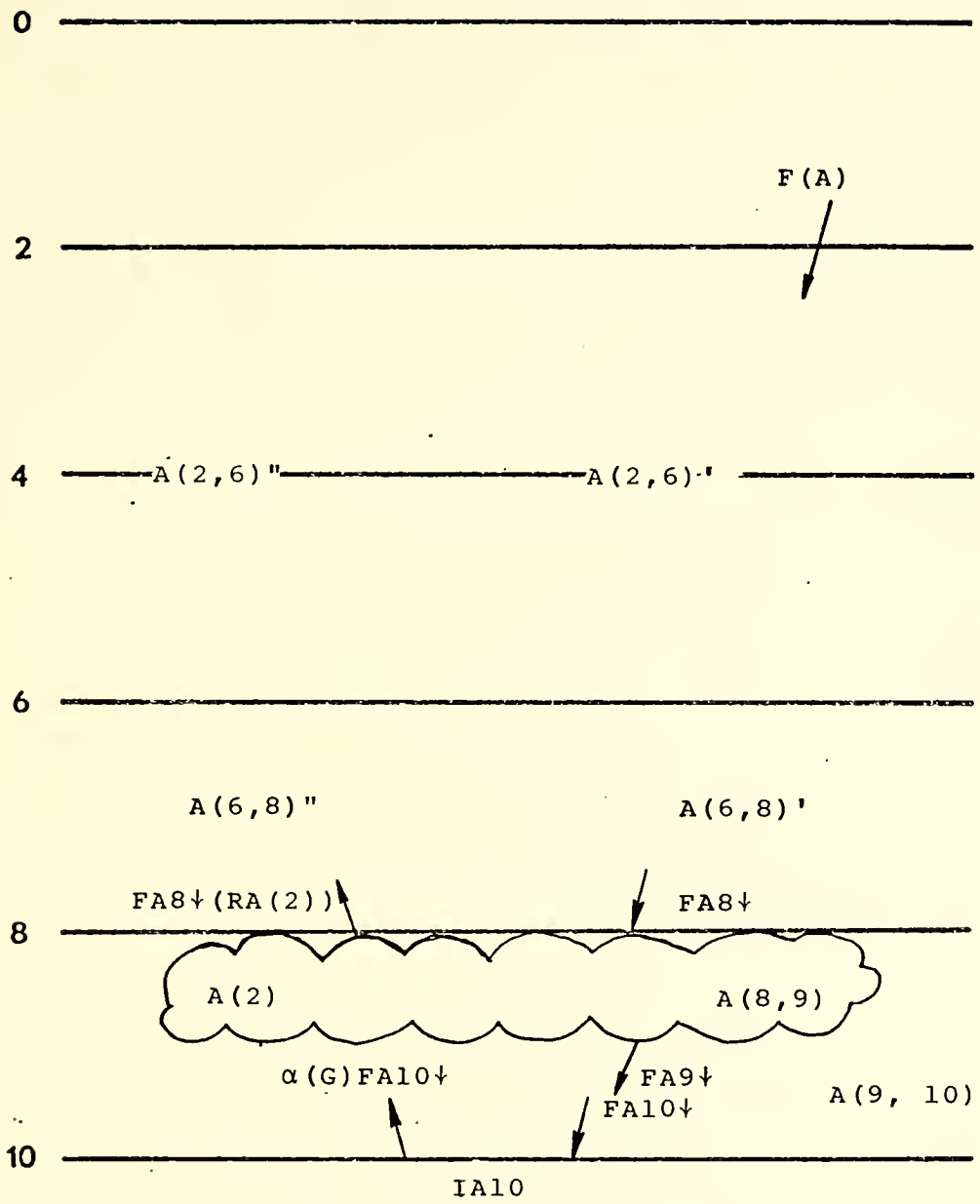

Figure 6. Schematic representation of F(A) insolation disposition with a lower overcast layer only.

$$A(2, 6)' = .271F(A)[U(2, 6)\text{Sec } Z]^{0.303} \quad (3\text{-}24a)$$

$$A(6, 8)' = .271F(A)[U(2, 8)\text{Sec } Z)^{0.303} - (U(2, 6)\text{Sec } Z)^{0.303}] \quad (3\text{-}24b)$$

$$FA8\downarrow = F(A)[1-.271(U(2, 8)\text{Sec } Z)^{0.303}] \quad (3\text{-}24c)$$

$$FA9\downarrow = FA8\downarrow[1-RA(2)-A(2)] \quad (3\text{-}24d)$$

$$FA8\uparrow = FA8\downarrow RA(2) \quad (3\text{-}24e)$$

$$A(6, 8)'' = FA8\downarrow[.271(U(6, 8)\text{Sec } Z)^{0.303}] \quad (3\text{-}24f)$$

$$A(6, 8) = A(6, 8)' + A(6, 8)'' \quad (3\text{-}24g)$$

$$A(2, 6)'' = .271FA8\uparrow[(U(2, 8)\text{Sec } Z)^{0.303} - (U(6, 8)\text{Sec } Z)^{0.303}] \quad (3\text{-}24h)$$

$$A(2, 6) = A(2, 6)' + A(2, 6)'' \quad (3\text{-}24i)$$

$$A(8, 9) = FA8\downarrow A(2) \quad (3\text{-}24j)$$

$$FA10\downarrow = FA9\downarrow TD(9, 10)[1-\alpha(G)RA(2)(TD(9, 10))^{2}]^{-1} \quad (3\text{-}24k)$$

$$A(9, 10) = FA9\downarrow - FA10\downarrow \quad (3\text{-}24\ell)$$

These variables also have similar definitions to those in Section III-C-2. As before the absorption by the earth's surface is given by

$$IA10(0, 1) = FA10\downarrow (1 - \alpha(G)) \quad (3\text{-}25)$$

5. Weighted F(A) Surface Insolation

As previously described in the section on the F(S) insolation, the values of IA10 calculated for the cases (0, 0), (1, 1), (1, 0) and (0, 1) must be appropriately weighted by the values described in Equation (3-12) in order to arrive at the composite F(A) surface-absorbed insolation.

$$IA10 = IA10(0, 0)W(0, 0) + IA10(1, 1)W(1, 1) + IA10(1, 0)W(1, 0) + IA10(0, 1)W(0, 1) \quad (3\text{-}26)$$

6. Atmospheric Layer Absorption of F(A)

In each of the four cases discussed, the F(A) insolation was absorbed as it passed through the key atmospheric layers (2, 6) and (6, 10). In the clear-sky case these absorptions are given by Equations (3-15) and (3-17). However, in the calculations of the cloudy-sky cases the various contributions have merely been added together to give the total insolation absorbed in the layer (2, 6) and then in the layer (6, 10), even though cloudiness affects the radiation physics differently within the cloud and subcloud layers as Figures 3, 4, 5, and 6 indicate.

a. Overcast in Both Cloud Layers

In this case the insolation absorbed in the two layers was calculated with values from the appropriate equations from (3-19a, ..., 3-19ℓ)

$$A(2, 6)_{1,1} = A(2, 4)' + A(2, 4)'' + A(4, 6)$$
$$A(6, 10)_{1,1} = A(6, 8) + A(8, 9) + A(9, 10) \quad (3\text{-}27)$$

where the subscript (1, 1) on A(6, 10) indicates the cloud layer combinations which will subsequently be weighted.

b. Upper Overcast Only

For the high level overcast only the insolation absorbed was calculated using the various equations

(3-22a, ..., 3-22e).

$$A(2, 6)_{1,0} = A(2, 4) + A(4, 6)$$
$$A(6, 10)_{1,0} = FA6\downarrow - FA10\downarrow \qquad (3\text{-}28)$$

c. Lower Overcast Only

In the low level overcast case the value of the insolation absorbed in the layers (2, 6) and (6, 10) was calculated using equations of (3-24a, ..., 3-24ℓ)

$$A(2, 6)_{0,1} = A(2, 6)' + A(2, 6)'' \qquad (3\text{-}29)$$
$$A(6, 10)_{0,1} = A(6, 8)' + A(6, 8)'' + A(8, 9) + A(9, 10)$$

d. Composite Weighted Absorption by Layers

In this case, as in the previous subsection on weighted F(A) surface insolation, the values computed in each of the four cases must be appropriately weighted by the functions described in Equation (3-12) in order to arrive at a composite value of the F(A) insolation absorbed in the atmospheric layers (2, 6) and (6, 10).

$$A(2, 6)=A(2, 6)_{0,0} W(0, 0)+A(2, 6)_{1,1} W(1, 1)$$
$$+A(2, 6)_{1,0} W(1, 0)+A(2, 6)_{0,1} W(0, 1) \qquad (3\text{-}30)$$
$$A(6, 10)=A(6, 10)_{0,0}W(0, 0)+A(6, 10)_{1,1}W(1, 1)$$
$$+A(6, 10)_{1,0}W(1, 0)+A(6, 10_{0,1}W(0, 1) \qquad (3\text{-}31)$$

e. The Absorptivity (ABA) by Layers

In this study it was convenient to deal with the fractional absorptivity, or simply absorptivity, as

well as the actual insolation energies absorbed in each layer, given by Equations (3-32 and 3-33) and by Equation (3-26) at the ground. In the calculation of the absorptivity, the total incoming insolation at the top of the atmosphere must be known. This value was calculated using Equation (3-32)

$$FADJ = 2.00(R/R_m)^{-2} \text{ Cos } Z \qquad (3\text{-}32)$$

Table II lists the instantaneous values of FADJ at each gridpoint along the three data lines. The calculation of the full-tropospheric absorptivity then follows from

$$ABA = \frac{A(2, 6) + A(6, 10)}{FADJ} \qquad (3\text{-}33)$$

which is the ratio of the insolation absorbed in the troposphere to the extraterrestrial insolation at the same time for each gridpoint.

D. REFLECTION OF F(A) AND F(S) ENERGY

In the calculations of the albedo and the fractional absorptivity of the ground both the F(A) and F(S) fractions of the solar insolation had to be considered.

1. Albedo

That portion of the F(A) insolation which was reflected back to space is given by

$$REFA = [F(A) - A(2, 6) - A(6, 10) - IA10] \qquad (3\text{-}34)$$

TABLE II. Total extraterrestrial insolation (FADJ) at each grid-point of the three data lines (ly min^{-1}).

Line 1	Line 2	Line 3
.899	1.899	1.346
.923	1.912	1.374
.947	1.923	1.403
.970	1.933	1.430
.995	1.939	1.458
1.018	1.946	1.485
1.042	1.947	1.510
1.064	1.947	1.534
1.085	1.942	1.558
1.106	1.934	1.579
1.125	1.923	1.597
1.142	1.907	1.613
1.158	1.888	1.626
1.171	1.862	1.634
1.180	1.834	1.638
1.187	1.798	1.637
1.190	1.757	1.629
1.187	1.710	1.616
1.181	1.658	1.593
1.168	1.598	1.565
1.149	1.534	1.526
1.122	1.462	1.478
1.088	1.384	1.419
1.048	1.301	1.350
.998	1.210	1.270

where the calculation equations of A(2, 6), A(6, 10), and IA10 have been described in Equations (3-30), (3-31), and (3-26), respectively.

The F(S) insolation reflected was simpler to calculate because the F(S) wavelengths do not undergo atmospheric absorption in the passage through the layers. The value of the reflected F(S) insolation is given by

$$REFS = F(S) - IS10 \tag{3-35}$$

where IS10 was calculated by Equation (3-13).

These values of REFA and REFS were then combined to give a value for REF, which is the total reflected energy passing outward through the tropopause (k=2)

$$REF = REFS + REFA \tag{3-36}$$

The albedo is defined as the ratio of the total reflected energy to the total incoming energy. This ratio was calculated by

$$ALB = \frac{REF}{FADJ} \tag{3-37}$$

where FADJ is defined in Equation (3-32). The values of REFA and REFS were computed at each grid-point. The resulting REF values are shown in cross-section form in Figures 11(a) and 11(b). Also, values of the albedo were computed. The global mean albedo over the 75 soundings turned out to be .412, based upon the cloud-cover parameterization for CL(1), CL(2).

2. Composite Absorptivity (ABG) by Earth

The total insolation absorbed at the earth was the sum of the weighted values of the F(S) and the F(A) portions of the incoming solar insolation.

$$Q(E) = IA10 + IS10 \qquad (3\text{-}38)$$

Here Q(E) is the insolation absorbed by the earth's surface at each grid-point sounding.

Using Q(E), a fractional absorptivity for the earth's surface was calculated. The equation used for the calculation was

$$ABG = \frac{Q(E)}{FADJ} \qquad (3\text{-}39)$$

where the calculations of Q(E) and FADJ have been previously discussed.

3. Check on Computations

The actual computational process used in this model was checked against the condition that the summation of the fractional values ALB, ABA, and ABG at each grid-point equals .96. This must be expected since we allowed for attenuation of the solar insolation in the amount of four percent as it passed through the stratosphere. This check computation was satisfied at each grid-point.

E. STATISTICAL COMPUTATIONS

1. Clear Sky Cases

In order to verify the preceding calculations, statistical computations of several key values were obtained

using linear regression techniques from the BMD set of statistical programs (Dixon, 1973). The predictand of the first computation was ALB (0,0,Z), which is the albedo in the clear sky case. The predictor was the secant of the zenith angle (Sec Z). The best-fit equation which resulted was

$$ALB(0,0,Z) = (-0.02726 + 0.11387 \text{ Sec } Z) \qquad (3\text{-}40)$$

with the regression coefficient R = .979. Equation (3-40) summarizes how the radiative model linearizes the effect of Sec Z in the clear sky case. The high R-value confirms the known result that Sec Z is a good predictor of the albedo (with clear skies), which is to be expected over an oceanic area. The mean albedo in the clear sky case, which corresponds to the average secant of the zenith angle, is as follows

$$\overline{ALB\ (0,\ 0)} = .135 \qquad \overline{Sec\ Z} = 1.428$$

Two other regressions that were performed using the linear regression technique were ABA (0,0,M) and ABG (0,0,M) against the water-vapor mass path length M, where M is given by

$$M = (U \text{ Sec } Z)^{1/2} \left[\log_{10} (U \text{ Sec } Z)^{1/2}\right]$$

This parameterization of the water vapor mass is essentially that of Hanson (1971), who used a similar absorber-mass

predictor in his empirical specification of ABA for both clear and partly cloudy skies. The resulting equations obtained with clear skies in this study for ABA (0,0,M) and ABG (0,0,M) were

$$\text{ABA}\ (0,0,M) = .096 + .031(U\ \text{Sec}\ Z)^{1/2}[\log_{10}(U\ \text{Sec}\ Z)^{1/2}]$$

$$R = .984 \qquad (3\text{-}41)$$

$$\text{ABG}\ (0,0,M) = .800 - .035(U\ \text{Sec}\ Z)^{1/2}[\log_{10}(U\ \text{Sec}\ Z)^{1/2}]$$

$$R = .956 \qquad (3\text{-}42)$$

The means and standard deviations of $\overline{\text{ABA}(0,0,M)}$, $\overline{\text{ABG}(0,0,M)}$, and $\bar{M}$, based on all of the original 75 soundings, are given below

$$\overline{\text{ABA}(0,0,M)} = .137 \qquad \sigma = .029$$

$$\overline{\text{ABG}(0,0,M)} = .687 \qquad \sigma = .034$$

$$\bar{M} = 1.342(\text{gm cm}^{-2})^{1/2} \qquad \sigma = .934\ .$$

2. Relationship between Albedo in the Cloudy and Clear Sky Cases

As discussed previously, it was possible to compute the value of ALB in the clear sky case and also in the composite cloudy sky case. In order to study the relationship between these two cases a ratio ALB[CL(I),CL(2)]/ALB(0,0) for the same zenith angle at grid point (I,J) was formed. This value was used as the predictand and the total opaque cloud cover (CL), specified by the model was used as the predictor. Here CL is calculated using Equation (3-43), which approximates the effective cloud-cover by the two

layers of clouds:

$$CL = CL(1) + CL(2) - CL(1)(CL(2) \quad (3\text{-}43)$$

The regression equation which resulted was

$$ALB[CL(1),CL(2)] = ALB(0,0)(1 + 3.931CL - .8782CL^2) \quad (3\text{-}44)$$

$$R = 0.956$$

The means and standard deviations of the values in Equation (3-44) are

$$\overline{ALB[CL(1),CL(2)]} = .412 \qquad \sigma = .431$$

$$\overline{ALB(0,0)} = .135 \qquad \sigma = .141$$

$$\overline{CL} = .680 \qquad \sigma = .742$$

Note that the mean cloudy sky albedo generated by the model is 3.211 times that of the meam clear sky albedo. The high value of the correlation coefficient (R = .956) indicates reliability of the indicated dependence upon CL. This global mean albedo of .412 is somewhat higher than that recently reported [ALB = .300] by Raschke et al (1973). However, the mean value reported here does not have an input from the polar latitudes. Raschke, et al suggest that perhaps the reduced cloud amounts (CL) recently reported in low latitudes would account for the reduction compared to that computed here by the parameterization Equation (2-13), after Smagorinsky.

3. Statistical Relationship between Ground Insolation in the Cloudy and Clear Sky Cases

In this section as in the preceding one a ratio $Y \equiv ABG(CL)/ABG(0, 0)$ was formed for each sounding case to determine the best-fit regression formula using CL as the independent variable. The formula which resulted was

$$Y \equiv ABG(CL)/ABG(0,0) = (1 - .66CL), \quad R = .999 \quad (3\text{-}45)$$

The ratio of $ABG(CL)/ABG(0, 0)$ is essentially the corresponding ratio of the transmissions received by a pyrheliometer. Quinn (1970) has summarized the empirical solar transmissivity formulas by many investigators and shows that some of the most reliable estimates are very nearly as formulated by Equation (3-45). For example, Budyko (1956) for the tropics lists

$$ABG(CL)/ABG(0, 0) = 1 - .655CL$$

and Kimball (1928) lists the corresponding ratio as

$$ABG(CL)/ABG(0, 0) = 1 - .71C$$

The mean statistics over the sample soundings gave

$$\overline{ABG(CL)} = .379$$

$$\overline{ABG(0, 0)} = .688$$

$$\overline{CL} = .680$$

4. Absorptivities in Air

Here the computed values of the ratio ABA(CL)/ABA(0, 0) were investigated by least squares with the result

$$ABA(CL)/ABA(0, 0) = 1 + .37863CL, \quad R = .781 \qquad (3\text{-}46)$$

with mean statistics for the 75-case population

$$\overline{ABA(CL)} = .169$$

$$\overline{ABA(0, 0)} = .137$$

$$\overline{CL} = .680$$

This indicates that the atmospheric absorptivity is somewhat enhanced with the cloud-model solar dispositions introduced. An increasing solar absorptivity with increasing cloud cover is in general agreement with Plante's results (1972) in a one-layer cloud model.

5. General Conclusions

The statistical relationships developed from the radiation model show consistency with results reported by other researchers. For example, Equation (3-41) gives ABA which closely fits Hanson's (1971) empirical results, and Equation (3-45) gives a ratio of transmittance which closely agrees with the empirical results of Budyko (1956) and Kimball (1928). Finally, the mean value of ABA in clear skies ($\overline{ABA}$ =.137) corresponds closely to the tropospheric mean absorptivity of 15 percent reported by London (1957).

IV. TERRESTRIAL RADIATION

A. THEORETICAL AND EMPIRICAL BASIS

Sasamori (1968) developed empirical formulas for computing emissivities for long-wave flux calculations associated with the NCAR General Circulation Model. These empirical emissivity formulas are matched to the values developed by Yamamoto (1952) from radiative transfer theory, which have also been built into his well-known Radiation Chart. This chart has proved to be quite accurate for computational purposes, and is used here as a schematic guide for integration of the radiative transfers through the various layers of interest in the soundings discussed in Section II.

For utilization in the FNWC heating package the necessary emissivity formulas of Sasamori are those which will lead to expressions for

F^*_{10} = net IR flux at earth

F^*_6 = net IR flux at level k = 6

F^*_2 = net IR flux at level k = 2

The differences $F^*_6 - F^*_{10}$ and $F^*_2 - F^*_6$ will then give the IR flux-divergence (i.e., cooling rates) in the layers (6, 10) and (2, 6), respectively. A workable scheme for making such computations is presented below for various combinations of cloud cover [CL(1), CL(2)].

For example, in order to compute

$$F^{*}_{10} = B_{10} - \int_{B=0}^{B_{10}} \varepsilon_{wc}(U, C, T)\, dB \qquad (4\text{-}1)$$

one must have a good representation of the emissivity ε_{wc} as a function of both water vapor and CO_2 absorber masses along the sounding, that is along the path of integration. Figure 7(a) illustrates the concept involved at level k = 10, with clear skies, where the hatched area represents the downward flux at k = 10. Here the radiative sounding is converted into emissivities as indicated in the figure. The hatched area denoted by

$$\int_{B=0}^{B_{10}} \varepsilon_{wc}\, dB$$

is then the key quantity to be evaluated. For this integral evaluation, Sasamori (1968) proposes emissivity formulations of the type

$$\varepsilon_{wc}(8, 10) = \left\{ .240 \log_{10}[U(8, 10)] + .622 \right\} + .07262 \left\{ (1. - .62556[U(8, 10) + .0286]^{.26}) * [\log_{10} C(8, 10) + 1.064] \right\} \qquad (4\text{-}2)$$

for temperatures $T \geq 210°K$, where ε_{wc} is very nearly temperature independent. The quantity in the first brace of Equation (4-2) indicates the water vapor emissivity alone, whereas that in the second brace is the added contribution by the part of the CO_2 emissivity transmitted through the water vapor "overlap" near 15 μm.

Equation (4-2) was used in the calculation of the atmospheric emissivities over any limits (6, 10), (4, 10), ... , (1, 10) for which running mass values U(6, 10), C(6, 10), etc. were available from the radiative soundings. Hence Equation (4-2) is extremely versatile in its applicability. In order to complete the integration from level k = 1 to the origin (B = 0, ε = 1.0), the $U(T_k)$, $C(T_k)$ soundings were taken as isothermal at $T = T_1$ over the layer (0, 1). However, it is still necessary, as Sasamori points out, to determine the hatched areas on the Yamamoto diagrams for the temperature-dependent emissivity $\tilde{\varepsilon}_{wc}[U(0, 10), T_1]$. This was computed after Sasamori as

$$\tilde{\varepsilon}_{wc}[U(0, 10), T_1] = 8.34T_1^{.353 \log_{10} U(0, 10) - .44} * U(0, 10)^{-.03455-.705 * [8.0/(.353 \log_{10} U(0, 10) + 3.56)]} + .07262\left\{ (1. - .62556[U(0, 10) + .0286]^{.26}) * [\log_{10} C(0, 10) + 1.064] \right\} \qquad (4\text{-}3)$$

The final term in the braces of Equation (4-3) involves essentially the same form of the CO_2 correction to the total emissivity as appeared in Equation (4-2). The first term in Equation (4-3) is, however, temperature-dependent, as well as dependent upon the summed absorber masses relative to the reference level (taken here as k = 10). It is clear that Equation (4-3) is applicable with appropriate final parameters U(0, k), C(0, k), and T_1, to the

determination of the curvilinear portion of the downward flux contribution through level k for all of the reference level cases to be considered below, e.g., k=2, 6.

B. NET FLUX F^*_{10}, WITH CLOUDY SKIES

The radiative soundings have been evaluated in the form of the parameters U(k, 10), C(k, 10), T_k, level for level. In addition there is listed for each radiative sounding at every grid-point the cloud-cover parameters CL(1) and CL(2), which in general are not both zero. The grid area may then be visualized as comprising the areal fractions W(0, 0), W(1, 1), W(1, 0), and W(0, 1) defined by Equation (3-12), of the following cases:

(a) totally clear skies, (case 0, 0)

(b) overcast in both layers, (case 1, 1)

(c) overcast in upper layer only, (case 1, 0)

(d) overcast in lower layer only, (case 0, 1)

The resultant radiative effect of the true cloud cover over the grid area is then reconstructed by multiplying the results of the respective cases by the appropriate weight factors. It is expedient to discuss first the totally clear sky case (Figure 7(a)).

1. Net Flux F^*_{10} with Clear Skies

If the hatched area $F\downarrow_{10}$ of Figure 7(a) is evaluated using the trapezoidal summation rule, then the net flux F^*_{10} becomes

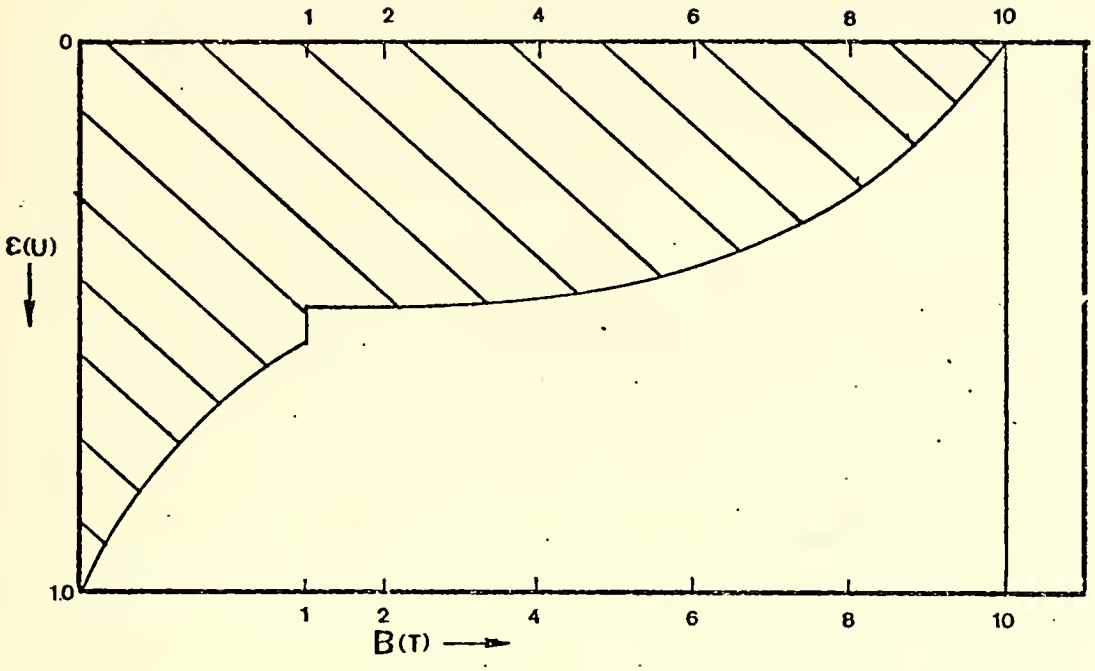

Figure 7(a). Terrestrial net flux F_{10}^{*} with clear skies, (case(0,0)). The unhatched area depicts

$$F_{10}^{*} = \int_{B=0}^{B_{10}} (1-\varepsilon_{wc})\, dB$$

$$F^*_{10} = B_{10} - .5\{\varepsilon_{wc}(8,10)(B_{10}-B_8)+(B_8-B_6)[\varepsilon_{wc}(6,10)$$

$$+\varepsilon_{wc}(8,10)]+[\varepsilon_{wc}(4,10)+\varepsilon_{wc}(6,10)](B_6-B_4)+(B_4-B_2)[\varepsilon_{wc}(2,10)$$

$$+\varepsilon_{wc}(4,10)]+[\varepsilon_{wc}(1,10)+\varepsilon_{wc}(2,10)](B_2-B_1)+\tilde{\varepsilon}_{wc}[(0,10),T_1]B_1\}$$

$$B_k = 1.170403 * 10^{-7}\ T_k^4\ \text{ly(day)}^{-1} \qquad (4\text{-}4)$$

Here B_k is the Stephen-Boltzman blackbody flux at T_k.

2. Net Flux F^*_{10} with Overcast Clouds in Both Layers

Here Figure 7(b) is converted into a numerical form using the Sasamori type emissivities [Equations (4-2), (4-3)] in the quadrature process. The result is

$$F^*_{10}(1,\ 1) = (B_{10} - B_9)[1. - .5\varepsilon_{wc}(9,\ 10)] \qquad (4\text{-}5)$$

where B_k is defined in Equation (4-4).

3. Net Flux F^*_{10} with Overcast Clouds in Upper Layer Only

Here Figure 7(c) is converted into a numerical form by the quadrature process after computing ε_{wc} using Equations (4-2) and (4-3). The result is

$$F^*_{10}(1,\ 0) = (B_{10}-B_6)\ \{1. - .5[\varepsilon_{wc}(8,\ 10)(B_{10}-B_6)$$

$$+[\varepsilon_{wc}(8,\ 10)+\varepsilon_{wc}(6,\ 10)](B_8-B_6)]\} \qquad (4\text{-}6)$$

The rationale of Equation (4-6) is that the downward flux is essentially B_6 plus an increment which is in the upper

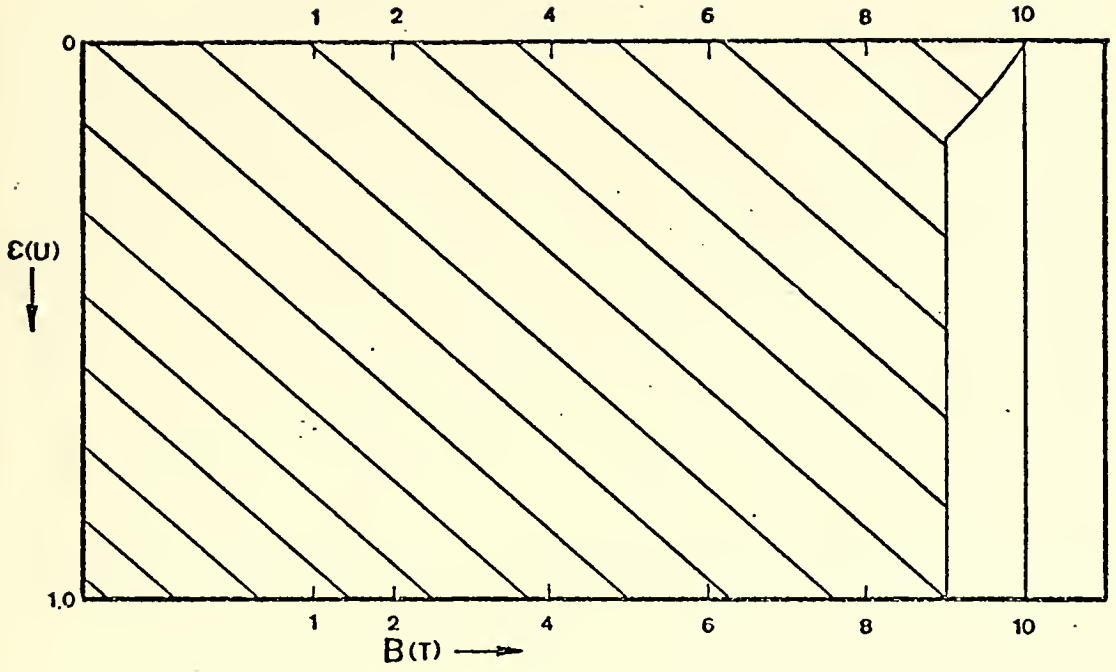

Figure 7(b). Terrestrial net flux F^*_{10} with both high and low level overcast cloud decks, ^{10}(case(1,1)). The unhatched area depicts

$$F^*_{10} = \int_{B=0}^{B_{10}} (1-\varepsilon_{wc})\, dB$$

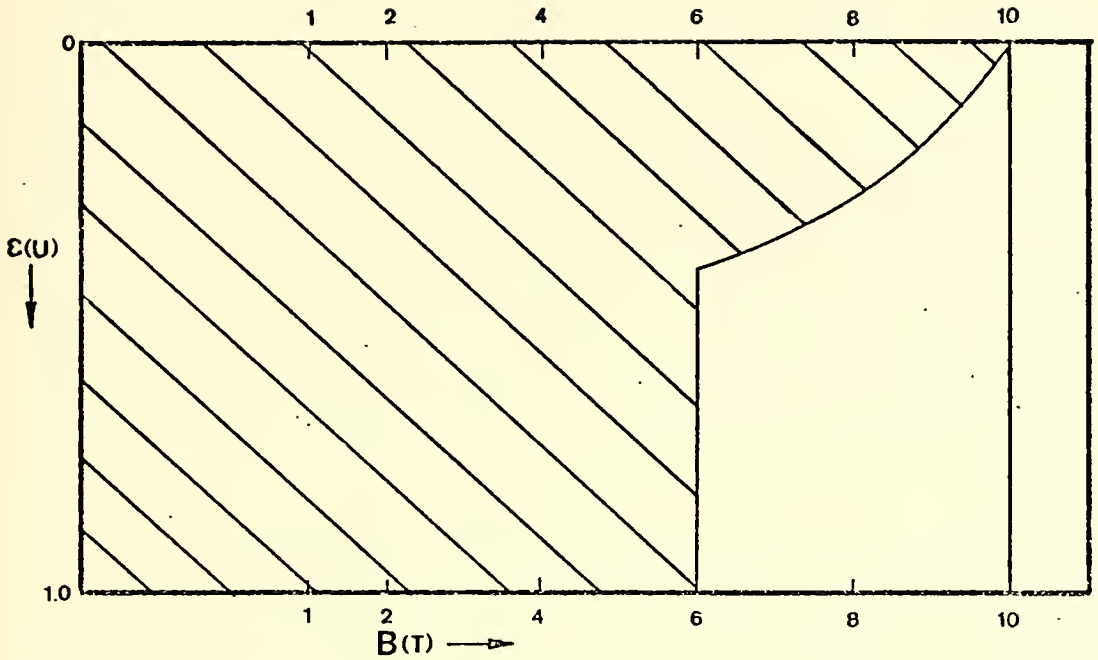

Figure 7(c). Terrestrial net flux F^{*}_{10} with high level overcast clouds in the layer k=4 to k=6 only, (case (1,0)). The unhatched area depicts

$$F^{*}_{10} = \int_{B=0}^{B_{10}} (1 - \varepsilon_{wc})\, dB$$

right corner of Figure 7(c), given by the summed combination of the products of the form

$$.5\ \varepsilon_{wc} * \Delta B$$

as these appear in the brackets in Equation (4-6).

4. Net Flux F^*_{10} with Overcast in Lower Layer Only

Here the numerical result follows immediately from the graphical depiction of Figure 7(d). This case becomes a replicate of the result of Section IV(B)2, with

$$F^*_{10}(0,1) = (B_{10} - B_9)[1. - .5\varepsilon_{wc}(9,10)] \qquad (4\text{-}7)$$

5. Composite F^*_{10} Calculations

Here we use the principle enunciated in Section IV (B), and express $F^*_{10}[CL(1), CL(2)]$ as the properly cloud-weighted sum of the respective results of cases (a), (b), (c), and (d). The result must have the form [see Equations (3-13) and (3-26)]

$$F^*_{10} = W(0,0)\ F^*_{10}(0,0) + W(1,1)\ F^*_{10}(1,1) + W(1,0)\ F^*_{10}(1,0) + W(0,1)\ F^*_{10}(0,1) \qquad (4\text{-}8)$$

with the cloud-weighted fractions, W(0,0), W(1,1), W(1,0) and W(0,1) defined in Section III(B)3. The composite result simplifies to

$$F^*_{10} = [1-CL(2)]\left\{ (B_{10} - B_6) - .5\ \varepsilon_{wc}(8,10)\ (B_{10} - B_8) + [\varepsilon_{wc}(8,10) + \varepsilon_{wc}(6,10)]\ (B_8 - B_6)\right\} +$$

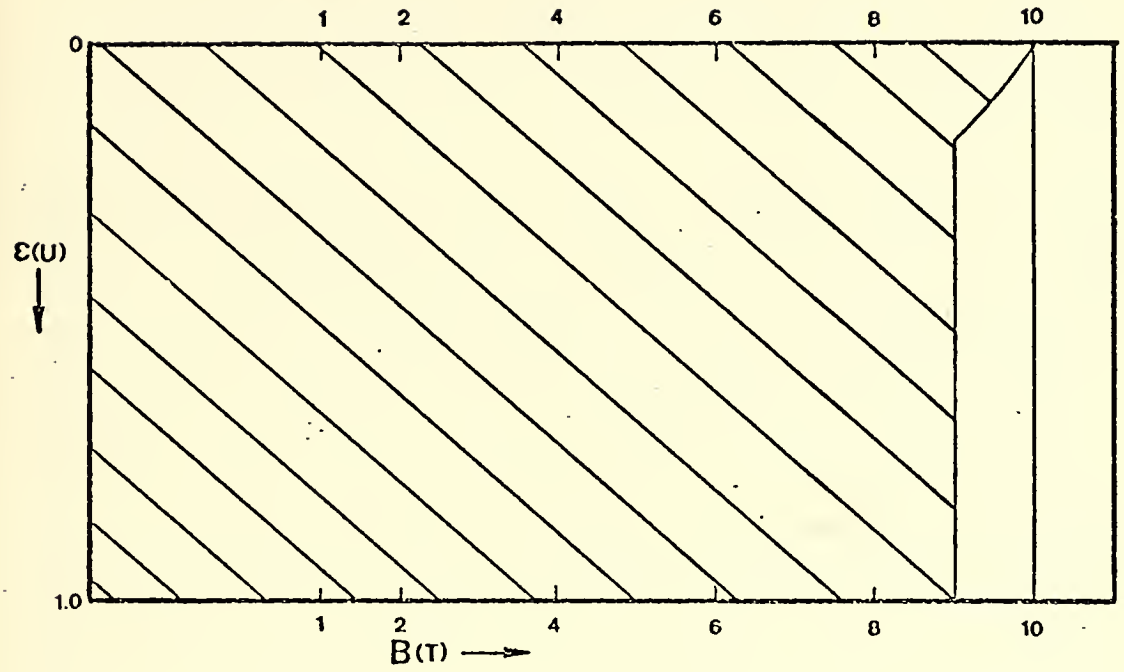

Figure 7(d). Terrestrial net flux F^{*}_{10} with low level overcast clouds in the layer k=8 to k=9 only, (case (0,1)). The unhatched area depicts

$$F^{*}_{10} = \int_{B=0}^{B_{10}} (1 - \varepsilon_{wc})\, dB$$

$$+(1-CL(2))(1-CL(1))\Big\{ B_6-.5\Big[(\varepsilon_{wc}(6,10)+\varepsilon_{wc}(4,10))(B_6-B_4)$$

$$+[\varepsilon_{wc}(4,10)+\varepsilon_{wc}(2,10)](B_4-B_2)+[\varepsilon_{wc}(2,10)+\varepsilon_{wc}(1,0)](B_2-B_1)$$

$$+\tilde{\varepsilon}_{wc}((0,10),T_1)\Big]\Big\} \quad +CL(2)\Big\{(B_{10}-B_9)[1.-.5\varepsilon_{wc}(9,10)]\Big\}$$

(4-9)

Note that Equation (4-9) reduces to $F^*_{10}(0,0)$ when CL(1) = CL(2) = 0, and to $F^*_{10}(1,1)$ when CL(1) = CL(2) = 1.0. Similarly the other two subcases of F^*_{10} may be recovered by setting up the weights corresponding to CL(1) = 1.0, CL(2) = 0.0 and CL(1) = 0.0, CL(2) = 1.0, respectively.

This procedure is similarly extended to levels k=6 and k=2. The results are as listed in the following subsections.

C. NET FLUX F^*_6 WITH CLOUDY SKIES

Formulation of expressions for the unhatched areas of Figures 8(a), (b), (c) and (d), with appropriate weight factors W(0,0), W(1,1), W(1,0), and W(0,1) applied, when summed lead at once to the following result:

$$F^*_6 = (1-CL(1))\Big\{B_8-.5[\varepsilon_{wc}(6,8)(B_8-B_6)+\varepsilon_{wc}(4,6)(B_6-B_4)$$

$$+[\varepsilon_{wc}(4,6)+\varepsilon_{wc}(2,6)](B_4-B_2)+[\varepsilon_{wc}(2,6)+\varepsilon_{wc}(1,6)](B_2-B_1)$$

$$+\tilde{\varepsilon}_{wc}((0,6),T_1)B_1]\Big\} + (1-CL(1))(1-CL(2))\Big\{(B_{10}-B_8)[1-$$

$$.5(\varepsilon_{wc}(6,8)+\varepsilon_{wc}(6,10))]\Big\}+ CL(1)\Big\{(B_8-B_6)[1-.5(\varepsilon_{wc}(6,8))]\Big\}$$

$$+CL(1)(1-CL(2))\Big\{(B_{10}-B_8)(1-.5[\varepsilon_{wc}(6,8)+\varepsilon_{wc}(6,10)])\Big\}$$

(4-10)

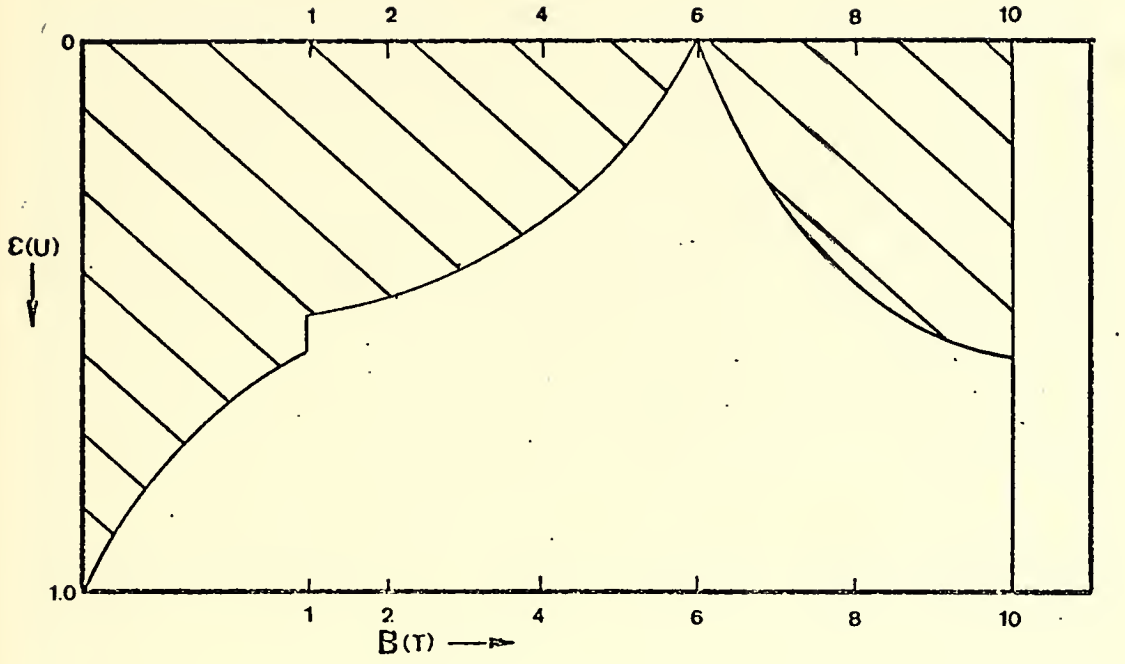

Figure 8(a). Terrestrial net flux F_6^*, with clear skies (case (0,0)). The unhatched area depicts

$$F_6^* = \int_{B=0}^{B_{10}} (1 - \varepsilon_{wc})\, dB \,.$$

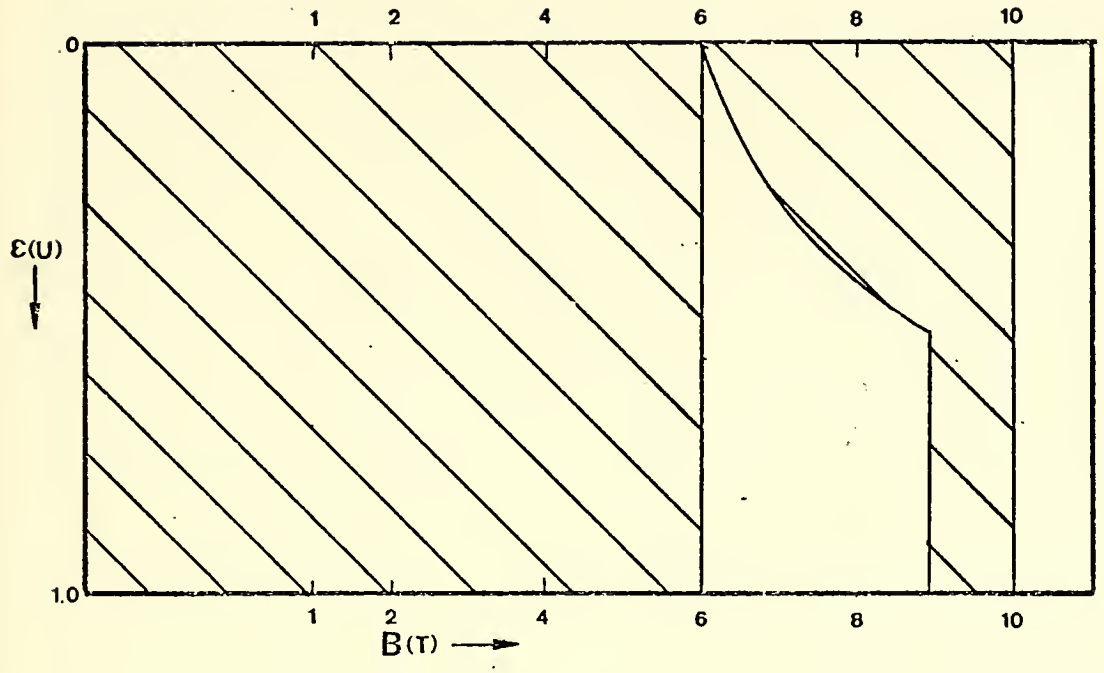

Figure 8(b). Terrestrial net flux F_6^*, with both high and low level overcast layers (case (1,1)). The unhatched area depicts

$$F_6^* = \int_{B=0}^{B_{10}} (1 - \varepsilon_{wc})\, dB$$

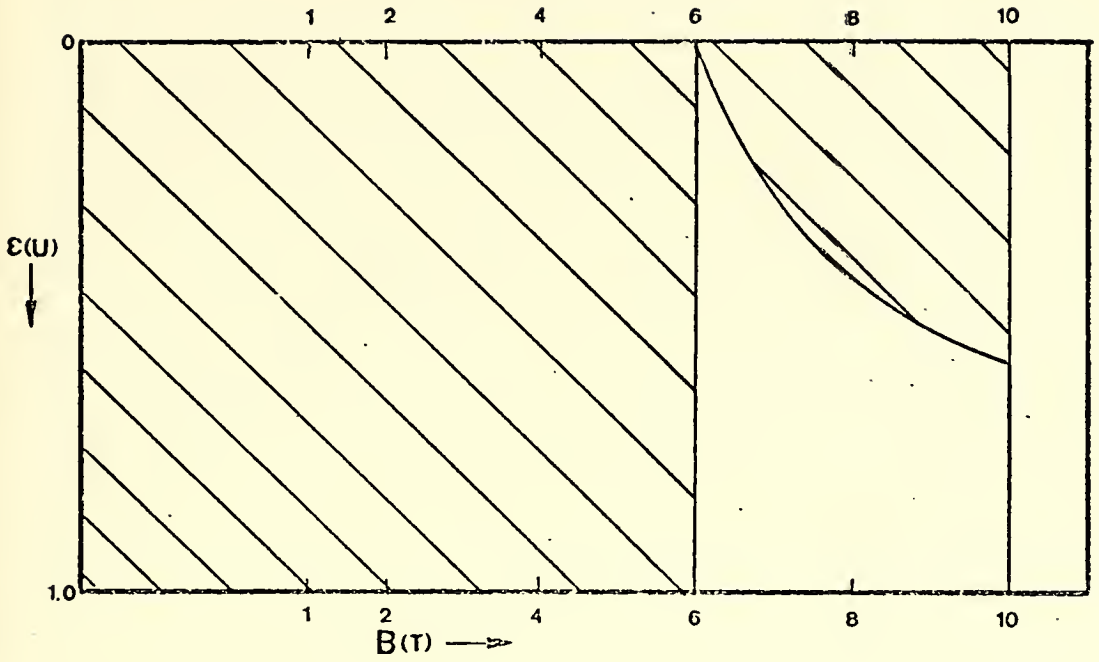

Figure 8(c). Terrestrial net flux F_6^*, with high level overcast clouds in the layer k=4 to k=6 only (case (1,0)). The unhatched area depicts

$$F_6^* = \int_{B=0}^{B_{10}} (1 - \varepsilon_{wc})\, dB$$

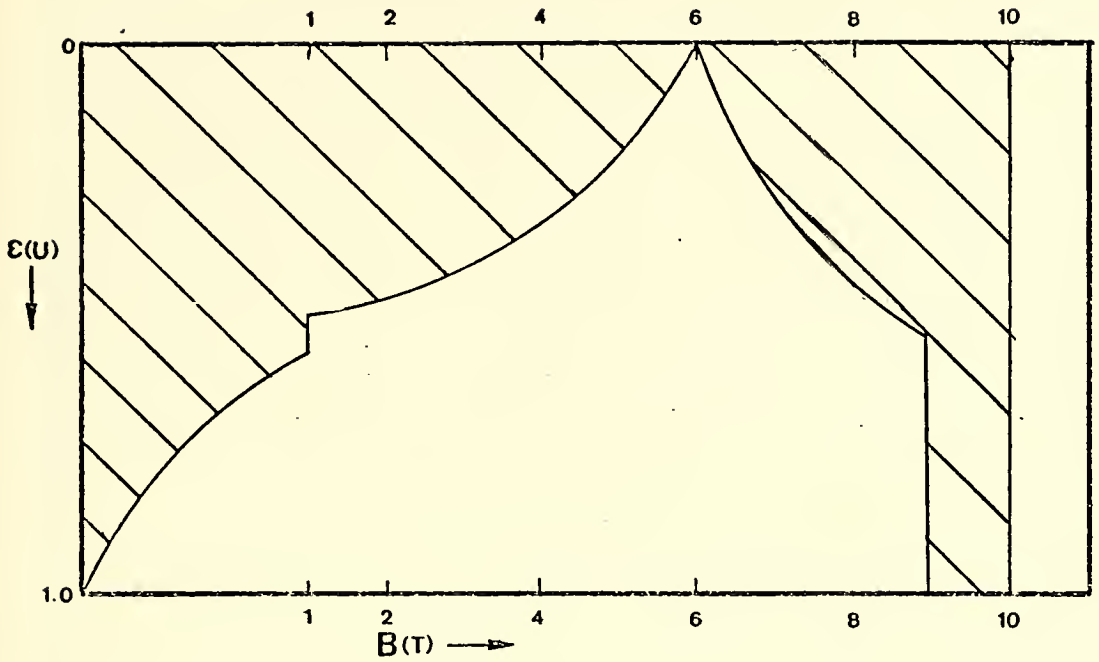

Figure 8(d). Terrestrial net flux F_6^*, with low level overcast clouds in the layer k=8 to k=9 only (case (0,1)). The unhatched area depicts

$$F_6^* = \int_{B=0}^{B_{10}} (1 - \varepsilon_{wc})\, dB$$

Equation (4-10) reduces to the properly formulated net fluxes for cloud cover cases (0,0), (1,1), (1,0), and (0,1) as these are depicted in Figures 8(a),(b),(c) and (d).

D. NET FLUX F_2^* WITH CLOUDY SKIES

Similar to F_{10}^* and F_6^* the net flux at level k=2 can be calculated using the trapezoidal rule. The net flux F_2^* is schematically depicted by the unhatched areas of Figures 9(a),(b),(c), and (d). After these areas have been calculated and weighted properly as described in the preceding two sections the following formula results

$$F_2^* = (1-CL(1))\{B_8 - .5[\varepsilon_{wc}(2,4)(B_4-B_2) + (\varepsilon_{wc}(2,4)+\varepsilon_{wc}(2,6))(B_6-B_4) + [\varepsilon_{wc}(2,6)+\varepsilon_{wc}(2,8)](B_8-B_6) + \varepsilon_{wc}(1,2)(B_2-B_1) + \tilde{\varepsilon}_{wc}((0,2),T_1)(B_1)]\} + (1-CL(1))(1-CL(2))\{(B_{10}-B_8)[1-.5(\varepsilon_{wc}(2,8)+\varepsilon_{wc}(2,10))]\} + CL(1)\{B_4 - .5[\varepsilon_{wc}(2,4)(B_4-B_2)+\varepsilon_{wc}(1,2)(B_2-B_1) + \tilde{\varepsilon}_{wc}((0,2),T_1)B_1]\} \quad (4\text{-}11)$$

This equation also reduces to the net fluxes for the four cloud cover cases (0,0), (1,1), (1,0), and (0,1) when the appropriate weight factors for the simplified cloud covers are set into Equation (4-11).

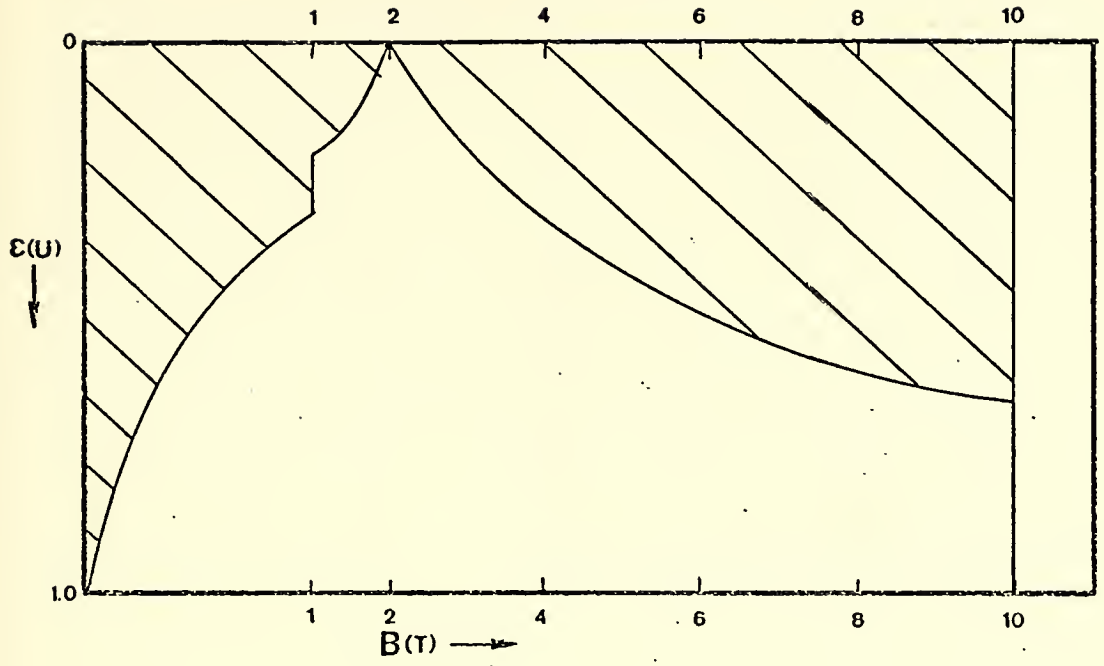

Figure 9(a). Terrestrial net flux F_2^*, with clear skies (case (0,0)). The unhatched area depicts

$$F_2^* = \int_{B=0}^{B_{10}} (1 - \varepsilon_{wc})\, dB$$

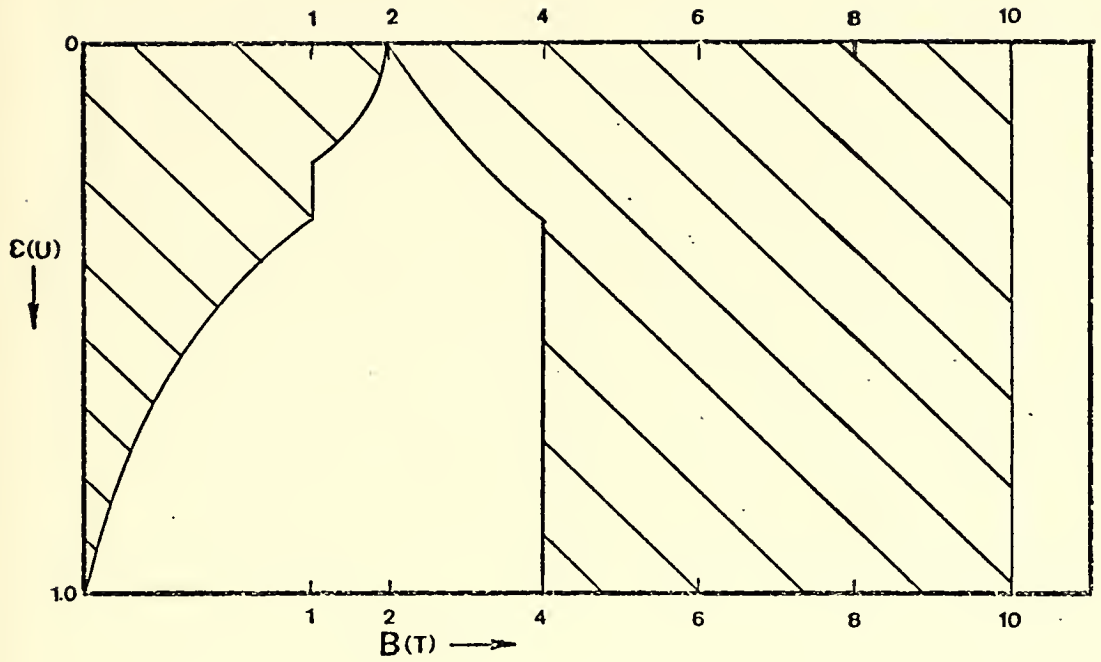

Figure 9(b). Terrestrial net flux F_2^*, with both high and low level overcast cloud decks (case (1,1)). The unhatched area depicts

$$F_2^* = \int_{B=0}^{B_{10}} (1 - \varepsilon_{wc})\, dB$$

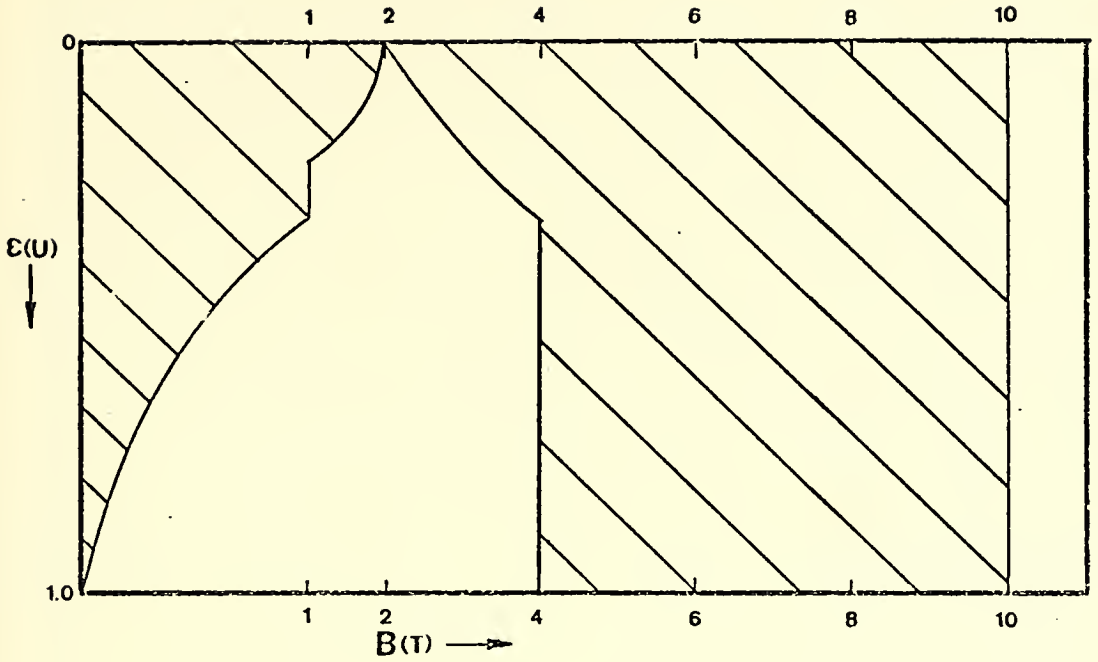

Figure 9(c). Terrestrial net flux with high level overcast clouds in the layer k=4 to k=6 only (case (1,0)). The unhatched area depicts

$$F_2^* = \int_{B=0}^{B_{10}} (1 - \varepsilon_{wc})\, dB$$

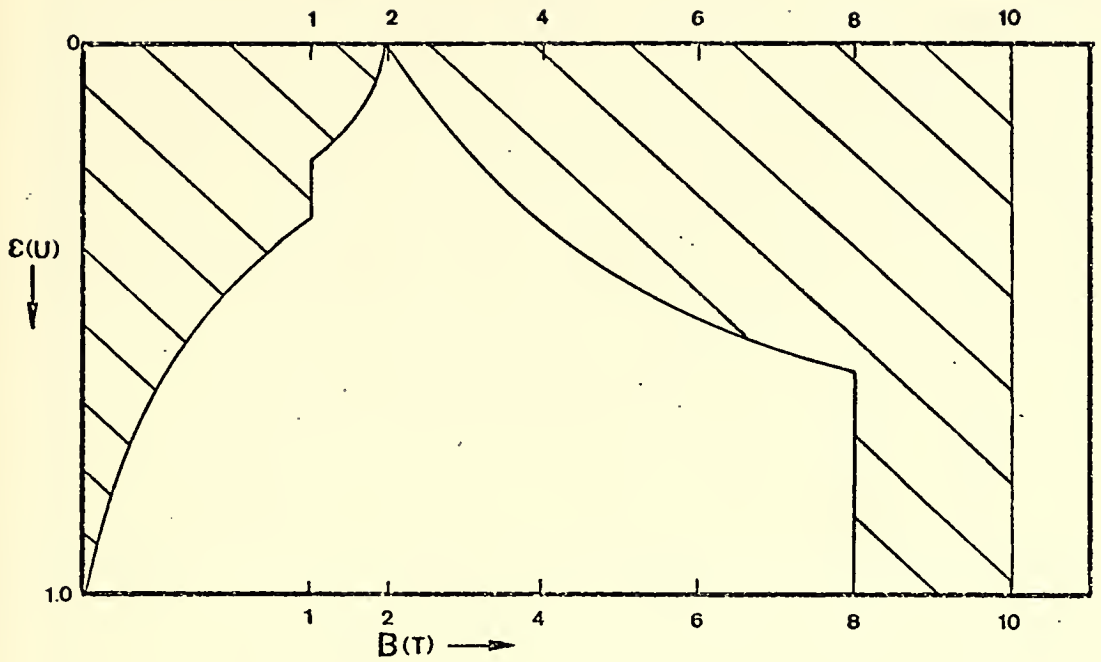

Figure 9(d). Terrestrial net flux F_2^*, with low level overcast clouds in the lower layer, k=8 to k=9, only (case (0,1)). The unhatched area depicts

$$F_2^* = \int_{B=0}^{B_{10}} (1 - \varepsilon_{wc})\, dB$$

E. APPLICATION TO HEAT BALANCE COMPUTATIONS

In computing the heat balance of the atmosphere, the layers (2,6) and (6,10) were considered to be undergoing solar heating (Section III). Now we require the long-wave cooling effects both instantaneously and averaged over the day (Section V). The long-wave cooling in (2,6) is symbolized by FU26 which is defined by

$$FU26 = F_2^* - F_6^*$$

Likewise that in (6,10) is symbolized by FU610 where

$$FU610 = F_6^* - F_{10}^*$$

is the flux-divergence in the lower half of the atmosphere.

For computations of the radiative "balance" at the tropopause only F_2^* of Equation (4-11) is required along with the net usable insolation. At the surface, a radiative balance is computed at each gridpoint involving the absorbed insolation and the net flux F_{10}^* of Equation (4-9), the latter considered a negative contribution. As will be seen in Section V, the long wave flux divergences FU26 and FU610 both act as destabilizing influences in their respective layers.

F. STATISTICAL RESULTS

1. Downward Flux with Clear Skies

Brunt (1932) demonstrated that the nighttime radiative measurements at the earth were expressible in a

statistical form

$$F_d = B_{10}(a + b\sqrt{e}) \qquad (4\text{-}12)$$

where B_{10} is the Stephen-Boltzman black body radiation ($B_{10} = St^*T_{10}^4$) at the surface, e is the water-vapor pressure in mb, and a and b are the regression coefficients, and $F_d \equiv B_{10} - F^*_{10}$. The regression coefficients referred to by Brunt were shown to be subject to wide variations depending on B_{10} and $\sqrt{e}$.

In this study a statistical test of Equation (4-12) was carried out by linear regression using a program from the BMD set of statistical programs (Dixon, 1973). The predictand selected for these computations was F^*_{10}, which included the downward contribution of CO_2 as well as that of water vapor on the calculation of the net flux at level 10. The statistical equation that resulted was

$$F^*_{10} = B_{10}(.30183 - .01314\sqrt{e}), \; R = .995 \qquad (4\text{-}13)$$

The correlation coefficient of Equation (4-13) shows that B_{10} and $B_{10}\sqrt{e}$ are good predictors of F^*_{10} and therefore of F_d. Using the values of a and b in Equation (4-13) and solving for F_d we obtain

$$F_d = B_{10}\left\{(1-a) - b\sqrt{e}\right\}$$

or

$$F_d = B_{10}(.69817 + .01314\sqrt{e}) \qquad (4\text{-}14)$$

The high value of the correlation coefficient indicates that Equation (4-13) may be regarded as an oceanic version of the Brunt F_d-equation. Note however that most of the dependence of F_d is with B_{10} and that the variation of F^*_{10} with $B_{10}\sqrt{e}$ is relatively slight. This is as to be expected over the ocean, where nearly constant relative humidities might well exist over large areas. The mean values of F_d and B_{10} for clear-sky cases are as listed below

$$\bar{F}_d = 637.09 \text{ ly day}^{-1}$$

$$\bar{B}_{10} = 843.47 \text{ ly day}^{-1}$$

so that $\bar{F}_d$ averages 75.5 percent of $\bar{B}_{10}$. These statistical averages are based upon the 57 grid-point soundings in the Northern Hemisphere only (those in the Southern Hemisphere have been deleted in order to eliminate tropical bias).

2. Statistical Relationship between Cloudy Sky and Clear Sky Cases

Based upon the radiative sounding parameters listed in Table I(b) and Equation (4-9) it was possible to compute $F^*_{10}[CL(1),CL(2)]$ and $F^*_{10}(0,0)$ based upon otherwise identical parameters.

For the purpose of this statistical study the ratio $F^*_{10}[CL(1),CL(2)]/F^*_{10}(0,0)$ was formed as the predictand, while an approximation to the composite total opaque cloud cover at the grid-point, defined in Equation (3-43) as

$$CL = CL(1) + CL(2)(1-CL(1))$$

for each cloudy sky case was used as the predictor. The simple regression formula based upon a best-fit to the 57 Northern Hemisphere data soundings became

$$F^*_{10}(CL) = F^*_{10}(0,0)(1 - .7575CL) \qquad (4\text{-}15)$$

with a regression coefficient, R = .983. A regression analysis using CL^2 as the predictor resulted in only a very small improvement of R. The hemispheric mean values of the various parameters in Equation (4-15) were as follows

$$\overline{F^*_{10}(CL)} = 112.48 \text{ ly day}^{-1}$$

$$\overline{F^*_{10}(0,0)} = 206.38 \text{ ly day}^{-1} \qquad (4\text{-}16)$$

$$\overline{CL} = 0.6103$$

Here the superior bar means the sample mean was taken over the 57 Northern Hemisphere grid-points.

The mean results of (4-16) indicate that the surface net flux is decreased by the ratio (93.9/206.38) = .455 with $\overline{CL}$ = 0.6103. This is to say that the downward flux $F_{d,10}$ is on the average 45.5 percent larger than with the clear-sky case for the cloud-parameterization of Equation (2-13).

3. F^*_2 (CL) Relative to $F^*_2(0,0)$

Here the statistical parameter sought is the predictand

$$Y \equiv \frac{F^*_2(CL)}{F^*_2(0,0)} \qquad (4\text{-}17)$$

where both numerator and denominator are computed directly from Equation (4-11) with (a) the known CL(1), CL(2) used in the numerator, and with (b) CL(1) = CL(2) = 0 in the denominator. The regression result was cast in the desired form

$$Y = 1 - A_1(CL) - A_2(CL)^2$$

with A_1, A_2 to be determined. The resulting regression equation was

$$Y = 1 - .0742(CL) - .1450(CL)^2 \qquad (4\text{-}18)$$

with a multiple correlation coefficient R = 0.9431, and a standard error of estimate .0529. The mean values of $F_2^*(CL)$, $F_2^*(0, 0)$, were

$$\overline{F_2^*(CL)} = 453.19 \text{ ly day}^{-1}$$

$$\overline{F_{10}^*(0, 0)} = 517.70 \text{ ly day}^{-1}$$

$$\overline{CL} = 0.6803$$

The mean $\overline{CL}$ here was based upon the 75 sounding-sample which contained a larger proportion of tropical cases than did those of the preceding section.

It is to be noted that the infrared loss to space has not been greatly impeded by the assumption of normal cloud cover since no thick cirrus clouds have been included in the model. With deep cirrus the "greenhouse effect" would be increased for gridpoint columns so affected.

For comparison with satellite long wave flux to space, which is usually given in ly min^{-1}, the foregoing F_2^* values should be divided by 1440 min day^{-1}.

Comparison with satellite measures of long wave flux should be made with $F_2\uparrow$ rather than with F_2^*, which includes a downward flux contribution from the stratosphere. For this purpose, computations were made with F_2^* of Equation (4-11) but omitting terms involving both levels "2" to "1" and "2" to "0", which are always associated with downward flux (see Figure 9). The comparison of the grid-point sounding mean $F_2[CL(1),CL(2)]$ was then made with the NIMBUS III global average long wave flux to space for the appropriate date (after Raschke et al, 1973). The comparison is as follows

$$F_2[CL(1), CL(2)] = .407 \text{ ly min}^{-1}$$

long-wave flux to space= .352 ly min^{-1} (after Raschke)

The comparison is quite good considering that the results of Raschke et al are Northern Hemisphere means for a two-week period in April 1969, whereas the results of this study, .407 ly min^{-1}, is essentially based upon a mid-Pacific cross-section on April 25th, which tends to be warmer than the globe as a whole.

V. MERIDIONAL CROSS-SECTIONAL DEPICTION OF RESULTS

In the computer programming of this model many outputs have been generated, so, for ease of examination of the output, an atmospheric cross-section along each of the three meridians studied was developed. This form of presentation was designed to give both the incoming and the outgoing radiations at the selected data levels. In addition, radiation balances were computed within key atmospheric layers and at the earth's surface at each gridpoint. In order to indicate the relevance of the cloud-amounts CL(1),CL(2) and CL to the resulting balances, these values were also plotted at appropriate levels (Figure 11, in parentheses) at gridpoints. These cross-sections were then interpolated to give the above results at five degree latitude gridpoints along the selected meridians. This was done for ease in calculation of a composite value of each of the computed radiative quantities at identical latitudes between 20°S and 65°N, wherever possible. Lines 1 and 3 extended from 20°S to 55°N and had identical latitude grid-points. Line 2 extended from the equator to 65°N and therefore permitted extension of the cross-section to 65°N. At latitudes south of the equator only two values were available for the composite computations and at latitudes higher than 55°N, only one value was available.

Between these extremes all three meridional cross-sections were used in the calculation of the composite case. Figure 11(a) and (b) depicts the composite cross-section with Figure 10 providing the key for locating the desired values.

In the cross-section to be depicted the insolation rates at level k=2, (QAVG) are given as averages over the 24-hour day (25 April 1973). This was done by employing Equation (3-1), but replacing Cos Z by $\overline{\overline{\text{Cos Z}}}$ where

$$\overline{\overline{\text{Cos Z}}} = [h \sin\phi \sin\delta + \cos\phi \cos\delta \sin h]/\pi \qquad (5\text{-}1)$$

and h = hour angle = Arc Cos$(-\tan\phi \tan\delta)$

ϕ = latitude

δ = declination (Smithsonian Tables (List, 1963))

Here the double bar over Cos Z represents a time mean over a 24 hour period, that is for a time period compatible with the long-wave flux transfers.

At each latitude a value of the instantaneous absorptivities, reflectivities or transmissivities was known for the time 0000GMT, and for the purpose of the cross-section presented here, these were assumed constant even though the insolation rates changed over the day. The IR transfer rates and their flux divergences were assumed to be constant both for the day and the composite grid-point as determined from their 0000GMT soundings. Thus it was possible to compute:

a) the earth-atmosphere radiative balance at level k=2 by the formula

$$QTROP = QAVG - (REFF + F_2^*) \qquad (5\text{-}2)$$

b) the radiative balance in the layer (2, 6) as given by

$$NET26 = ABS26 + FU26 \qquad (5\text{-}3)$$

c) the radiative balance in the layer (6, 10) as given by

$$NET610 = ABS610 + FU610 \qquad (5\text{-}4)$$

d) the radiative balance at the earth's surface as given by

$$NETSFC = ABSFC + F_{10}^* \qquad (5\text{-}5)$$

In addition to these mean grid-point items the cloud covers CL(1), CL(2) and (CL) in parentheses are depicted in the applicable layer after averaging to the grid-point. At the tropopause, and at the earth's surface a global average of radiative balance or net was obtained by cosine weighting as follows

$$\bar{Q} = \frac{\sum Q(\phi_i) \text{ Cos } \phi_i}{\sum \text{ Cos } \phi_i} \qquad (5\text{-}6)$$

where $Q(\phi_i)$ is the radiative net value under consideration at latitude ϕ_i. Some of these values are contrasted with

the other climatological results cited below

	This Study	Other Data
1) global balance at the tropopause	.048	.061, Raschke
2) global balance at the surface	.166	.140, Budyko

The outgoing long wave radiation in these computations was also in excellent agreement with that of Raschke et al (1973) as noted in Section IV. The global balance of total radiation at the tropopause is less than that reported by Raschke et al for the same general time of year. However, it was noted that this result primarily reflects the smaller value of planetary albedo (ALB = .300) reported from satellite observations.

Another set of results for comparison with those calculated here are due to Budyko (1956). Budyko calculated the radiation balance at the surface for ten-degree latitude bands. In his study, these values were taken for the balance at mid-points of these bands and compared with the computed output from the present model. The following table shows this comparison.

	This Study	Budyko (Longitude 180°)
5°N	.158	.203
15°N	.205	.209
25°N	.236	.190
35°N	.201	.148
45°N	.119	.103
55°N	.144	.064

All of the above values are in cal cm^{-2} min^{-1}. These comparisons would have been in closer agreement if the results of this study had been in the form of an annual average as Budyko's results were.

LAT.		
	Lat.	latitude of the grid-points in 5° increments
	a) QAVG	insolation averaged over 24 hours at k=2
	b) REFF	reflected insolation at k=2 (negative sign indicating loss)
	c) F_2^*	net upward long wave flux at k=2 (negative sign for outgoing)
2	d) NETROP	indicates net earth-tropospheric gain or loss (a+b+c)
	e) ABS26	solar insolation absorbed by layer (2, 6)
	(CL(1))	fractional high cloud cover
	f) FU26	IR flux loss between the indicated levels
	g) NET26	indicates warming or cooling in layer (2, 6), (e+f)
	(CL)	total opaque cloud amount, by Equation (3-43)
6		
	h) ABS610	solar insolation absorbed by layer (6, 10)
	(CL(2))	fractional low cloud cover
	i) FU610	IR flux loss between the indicated levels
	j) NET610	indicated warming or cooling in layer (6, 10), (h+i)
10		
	k) ABSFC	total solar insolation absorbed by surface
	l) F_{10}^*	net flux at the earth's surface k=10, considered as a cooling rate
	m) NETSFC	indicates net warming or cooling of earth (k=1)

Figure 10. Key to mean meridional cross-sections. All radiative values are in cal cm^{-2} min^{-1} for the levels or layers under consideration.

LAT.	-20	-15	-10	-5	0	5	10	15	20
	0.482	0.515	0.543	0.568	0.589	0.605	0.617	0.625	0.628
	-0.249	-0.207	-0.273	-0.293	-0.252	-0.258	-0.220	-0.210	-0.213
	-0.279	-0.272	-0.270	-0.272	-0.306	-0.322	-0.365	-0.373	-0.383
2	-0.046	-0.025	0.001	0.004	0.031	0.024	0.032	0.041	0.032
	0.055	0.062	0.067	0.069	0.062	0.056	0.048	0.042	0.039
	(0.67)	(0.71)	(0.75)	(0.75)	(0.51)	(0.42)	(0.18)	(0.19)	(0.09)
	-0.142	-0.146	-0.149	-0.152	-0.135	-0.131	-0.120	-0.118	-0.112
	-0.087	-0.085	-0.082	-0.082	-0.074	-0.075	-0.073	-0.076	-0.074
6	(0.89)	(0.91)	(0.89)	(0.91)	(0.74)	(0.75)	(0.58)	(0.53)	(0.53)
	0.038	0.039	0.039	0.042	0.051	0.059	0.071	0.070	0.074
	(0.66)	(0.66)	(0.56)	(0.62)	(0.49)	(0.54)	(0.51)	(0.43)	(0.47)
	-0.063	-0.081	-0.074	-0.082	-0.108	-0.127	-0.165	-0.161	-0.178
	-0.025	-0.042	-0.035	-0.040	-0.058	-0.067	-0.094	-0.091	-0.105
10									
	0.129	0.134	0.152	0.152	0.215	0.222	0.273	0.299	0.297
	-0.074	-0.044	-0.047	-0.038	-0.061	-0.064	-0.079	-0.094	-0.092
	0.056	0.090	0.105	0.114	0.154	0.158	0.194	0.205	0.206

Figure 11(a). Mean Meridional Cross section, tropical section.

LAT.	25	30	35	40	45	50	55	60	65
	0.626	0.620	0.610	0.596	0.577	0.555	0.530	0.502	0.472
	-0.164	-0.189	-0.238	-0.253	-0.298	-0.277	-0.237	-0.180	-0.109
	-0.400	-0.362	-0.317	-0.299	-0.282	-0.269	-0.270	-0.280	-0.256
2									
	0.062	0.068	0.055	0.044	-0.003	0.009	0.022	0.042	0.106
	0.032	0.039	0.044	0.043	0.042	0.039	0.031	0.018	0.020
	(0.00)	(0.18)	(0.31)	(0.36)	(0.36)	(0.28)	(0.23)	(0.00)	(0.14)
	-0.103	-0.110	-0.112	-0.114	-0.110	-0.105	-0.089	-0.075	-0.067
	-0.070	-0.071	-0.068	-0.071	-0.069	-0.068	-0.058	-0.057	-0.047
6	(0.31)	(0.39)	(0.55)	(0.64)	(0.88)	(0.91)	(0.73)	(0.54)	(0.17)
	0.067	0.055	0.049	0.051	0.060	0.060	0.050	0.048	0.017
	(0.31)	(0.33)	(0.53)	(0.57)	(0.82)	(0.75)	(0.67)	(0.54)	(0.04)
	-0.154	-0.143	-0.134	-0.121	-0.125	-0.120	-0.124	-0.132	-0.084
	-0.104	-0.089	-0.085	-0.069	-0.066	-0.060	-0.074	-0.084	-0.067
10									
	0.361	0.334	0.273	0.239	0.165	0.168	0.201	0.247	0.322
	-0.126	-0.109	-0.071	-0.064	-0.046	-0.044	-0.057	-0.072	-0.107
	0.236	0.225	0.201	0.175	0.119	0.124	0.144	0.175	0.215

Figure 11(b). Mean Meridional Cross-section, higher latitude section.

VI. CONCLUSIONS

Using three meridional lines of soundings over the Pacific Ocean a radiative model for inclusion in the FNWC numerical weather prediction scheme was evaluated. These three meridians of data-soundings were used to compute a space-time average of the radiational parameters for one day over the Pacific Ocean. This space-time average agreed fairly well with values derived from other studies, including satellite measurements. There were some minor differences which could be ascribed to the fact that the data used in this experiment was a one day space-time average while the comparison data was an average of several weeks for the satellite data, and over years in the case of surface climatological data.

Differences could also be induced by the parameterization of cloud amounts as well as by the treatment of cloud reflectivity and absorptivity for solar wavelengths. In this model, only two layers of clouds were considered and the same empirical values of the reflectivities and absorptivities were used for all latitudes, which could cause discrepancies when compared with satellite data.

Although the results of this data treatment agree fairly well with climatological comparisons cited at the end of Section V, refinements may be possible in the present model. This model should be tested using data

at different seasons of the year and over varying locales. With a full year of sampling, refinements in the cloud parameterization, atmospheric absorption values and reflection treatments could be developed for accurate use in the FNWC predictive model.

LIST OF REFERENCES

1. Arakawa, A., 1972: Design of the UCLA General Circulation Model, Numerical Simulation of Weather and Climate Tech. Rpt. No. 7, Department of Meteorology, University of California.

2. Brunt, D., 1939: Physical and Dynamical Meteorology, Cambridge University, London, 428 pp.

3. Budyko, M. I., 1956: The Heat Balance of the Earth's Surface, Leningrad, pp 255 (Translated by N. A. Slepanova; translation distributed by U. S. Weather Bureau, Washington, D. C.)

4. Coulson, K. L., 1959: Radiative Flux from the Top of a Rayleigh Atmosphere, Ph.D. Dissertation, Department of Meteorology, University of California, pp 60.

5. Crow, E. L., Davis, F. A., and Maxfield, M. W., 1955: Statistics Manual, pp 288, NAVORD REPORT 3369.

6. Davis, P. A., 1963: "An Analysis of the Atmospheric Heat Budget," Journal of the Atmospheric Sciences, Vol. 20, pp 5-22.

7. Dixon, W. J., 1973: Biomedical Computer Programs, University of California Press, pp 773.

8. Fleagle, R. G., Businger, J. A., 1963: An Introduction to Atmospheric Physics, Academic Press, New York, pp 346.

9. Gates, W. L., Batten, E. S., Kahle, A. B., and Nelson, A. B., 1971: A Documentation of the Mintz-Arakawa Two-Level Atmospheric Circulation Model, Advance Research Projects Agency Report No. R-877-ARPA, Rand Corporation, Santa Monica, California, 408 pp.

10. Hanson, K. J., 1971: Studies of Cloud and Satellite Parameterization of Solar Irradiance at the Earth's Surface, paper presented at the Miami Workshop on Remote Sensing, Miami, Florida, 29-31 March 1971.

11. Katayama, A., 1966: "On the Radiation Budget of the Troposphere over the Northern Hemisphere (I)," Journal of the Meteorological Society of Japan, Vol. 44, No. 6, pp 381-401.

12. List, R. J., 1958: Smithsonian Meteorological Tables, Smithsonian Institute, Washington, pp 527.

13. Malkus, J. S., 1962: "Large Scale Interactions," The Sea, Vol. 1, Interscience Publishers.

14. Martin, F. L. and Palmer, W. C., 1964: "Statistical Estimates of Computed Water-Vapor Radiative Flux from Clear Skies at an Oceanic Location," Journal of Applied Meteorology, Vol. 3, No. 6, pp 780-787.

15. Martin, F. L., 1972: Description of a Radiation Package for the Naval Postgraduate School General Circulation Model, Department of Meteorology, Naval Postgraduate School, Monterey, California.

16. Martin, F. L., 1974: Unpublished manuscript, Department of Meteorology, Naval Postgraduate School, Monterey, California.

17. Moller, F. and Raschke, E., 1964: Evaluation of TIROS III Radiation Data, National Aeronautics and Space Administration Contractor Rpt, NASA CR-112, Washington, D. C., 114 pp.

18. Pierson, W. J., and Neuman, G., 1966: Principles of Physical Oceanography, Prentice-Hall, pp 576.

19. Plante, R. J., 1973: Tests of a Radiative Transfer Model for Numerical Prediction of the Atmospheric General Circulation, M.S. Thesis, Department of Meteorology, Naval Postgraduate School, Monterey, California, 115 pp.

20. Quinn, W. H., 1971: Studies of Parameterization of Solar Irradiance at the Earth's Surface, paper presented at the Miami Workshop on Remote Sensing, Miami, Florida, 29-31 March 1971.

21. Raschke, E., Von Der Haar, T., Bandeen, W., Pasternak, M., 1973: "The Annual Radiation Balance of the Earth-Atmosphere System during 1969-70 from NIMBUS III Measurements," Journal of the Atmospheric Sciences, Vol. 30, No. 3, pp 341-364.

22. Sasamori, T., 1968: "The Radiative Cooling Calculation for Application to General Circulation Experiments," Journal of Applied Meteorology, Vol. 7, No. 5, pp 721-729.

23. Smagorinsky, J., 1960: "On the Dynamical Prediction of Large Scale Condensation by Numerical Methods," Geophysical Monograph, No. 5, American Geophysical Union, Washington, D. C., pp 71-78.

24. Yamamoto, G., 1952: On a Radiation Chart, Science Repts. of the Tohoku Univ., Series No. 5, pp 9-23.

INITIAL DISTRIBUTION LIST

		No. Copies
1.	Defense Documentation Center Cameron Station Alexandria, Virginia 22314	2
2.	Library, Code 0212 Naval Postgraduate School Monterey, California 93940	2
3.	Professor F. L. Martin, Code 51Mr Department of Meteorology Naval Postgraduate School Monterey, California 93940	6
4.	Lieutenant Frank W. Jenks III, USN 7048 Dayton Road Enon, Ohio 45323	3
5.	Department of Meteorology, Code 51 Naval Postgraduate School Monterey, California 93940	1
6.	Assistant Professor R. L. Haney, Code 51Hy Department of Meteorology Naval Postgraduate School Monterey, California 93940	1
7.	Naval Weather Service Command Naval Weather Service Headquarters Washington Naval Yard Washington, D. C. 20390	1
8.	Naval Oceanographic Office Library (Code 3330) Washington, D. C. 20373	1
9.	Commanding Officer Fleet Numerical Weather Central Monterey, California 93940	1
10.	Commanding Officer Environmental Prediction Research Facility Monterey, California 93940	1

SECURITY CLASSIFICATION OF THIS PAGE (When Data Entered)

REPORT DOCUMENTATION PAGE

READ INSTRUCTIONS BEFORE COMPLETING FORM

1. REPORT NUMBER	2. GOVT ACCESSION NO. / 3. RECIPIENT'S CATALOG NUMBER
4. TITLE (and Subtitle): Radiative Parameterization for the FNWC Global Primitive Equation Model	5. TYPE OF REPORT & PERIOD COVERED: Master's Thesis, March 1974
	6. PERFORMING ORG. REPORT NUMBER
7. AUTHOR(s): Frank Wright Jenks III	8. CONTRACT OR GRANT NUMBER(s)
9. PERFORMING ORGANIZATION NAME AND ADDRESS: Naval Postgraduate School, Monterey, California 93940	10. PROGRAM ELEMENT, PROJECT, TASK AREA & WORK UNIT NUMBERS
11. CONTROLLING OFFICE NAME AND ADDRESS: Naval Postgraduate School, Monterey, Califcrnia 93940	12. REPORT DATE: March 1974
	13. NUMBER OF PAGES: 89
14. MONITORING AGENCY NAME & AOORESS(if different from Controlling Office): Naval Postgraduate School, Monterey, California 93940	15. SECURITY CLASS. (of this report): Unclassified
	15a. DECLASSIFICATION/OOWNGRAOING SCHEOULE

16. OISTRIBUTION STATEMENT (of this Report)

Approved for public release; distribution unlimited.

17. DISTRIBUTION STATEMENT (of the abstract entered in Block 20, if different from Report)

18. SUPPLEMENTARY NOTES

19. KEY WORDS (Continue on reverse side if necessary and identify by block number)

Pressure scaled absorber mass
Atmospheric absorptivity
Earth absorptivity
Insolation

20. ABSTRACT (Continue on reverse side if necessary and identify by block number)

This study was an evaluation of a radiational scheme for inclusion in a numerical weather prediction model. This scheme uses empirical formulations for atmospheric absorptivities, scattering and reflectivity and cloud and earth surface reflectivity to compute the solar insolation received and absorbed by the earth and key atmospheric layers. Longwave cooling by the earth is also

DD FORM 1 JAN 73 1473 EDITION OF 1 NOV 65 IS OBSOLETE
S/N 0102-014-6601 |
(Page 1)

SECURITY CLASSIFICATION OF THIS PAGE (When Data Entered)

treated with empirically derived emissivities for water-vapor and carbon dioxide. This radiation model includes a two-layer cloud parameterization scheme and calculates the effect of an additional cloud layer on previous studies.

In testing the validity of this model, use was made of Fleet Numerical Weather Central data in the form of vertical soundings on a spring day over the ocean. This data was used to calculate the radiation balance at the tropopause, the earth's surface and the key layers of the atmosphere.

Thesis
J463
c.1

148629

Jenks
Radiative parameterization for the FNWC global primitive equation model.